Quantitative Laser-based Assessment of Top of Rail Friction Modifiers for Railroad Application

Abdullah Mohammed Hasan

Dissertation submitted to the faculty of the Virginia Polytechnic Institute and State University in partial fulfillment of the requirements for the degree of

Doctor of Philosophy
In
Mechanical Engineering

Mehdi Ahmadian, Co-Chair
Brian Vick, Co-Chair
Dong S. Ha
John M. Kennedy
Steve C. Southward

March 25th, 2016
Blacksburg, Virginia

Keywords: Tribology, Lubrication, Friction, Wear, Laser

Quantitative Laser-based Assessment of Top of Rail Friction Modifiers for Railroad Application

Abdullah Mohammed Hasan

Abstract

The primary purpose of this study is to assess the effectiveness and utility of laser-based sensors for measuring, quantitatively, the presence and extent of top-of-rail (TOR) friction modifiers that are commonly used in the railroad industry for reducing friction between railcar wheels and rail. Modifying the friction between the wheel and rail is not only important for significantly reducing rolling resistance, but it also contributes to reducing wheel and rail wear, lowering rolling contact fatigue, and potentially curving resistance. It is common to monitor rail lubrication empirically by manually observing the sheen of the rail and tactically sensing any residues that may be present on the rail. Often performed by experienced railroad engineers, such methods are highly subjective and do not provide a quantitative assessment of how lubricated or unlubricated the track may be.

A new, quantitative measurement method for accurately assessing the state of lubrication of rail is developed and studied in depth. The method takes advantage of the light reflection and dispersion properties of laser-based optical sensors to provide a repeatable, verifiable, and accurate measure of the presence of TOR friction modifiers on the rail. The measurement system is assembled in a self-contained, portable rail cart that can be pushed on the rail at walking speeds.

Various TOR states are assimilated in the lab for assessing the effectiveness of the laser system. Additionally, the laboratory results are repeated in the field on various tracks, including revenue service track. The results of the tests indicate that the developed system is able to accurately measure the presence of TOR friction modifiers from none to fully-saturated, but is not affected by environmental factors such as rain, sunlight, type of rail, and top-of-rail condition. The measurements provide the means for classifying the state of rail friction in an indexed manner. The results of the study will not only have a significant effect on more efficient use of TOR friction modifiers for promoting better fuel efficiency, but they can also have a major impact on braking practices in applications such as Positive Train Control (PTC).

To my family

Acknowledgments

I may not be the best person to describe his feelings, but the guidance, continuous support, and patience that helped me overcome many difficult situations make me grateful and incredibly fortunate to have an advisor like Professor Mehdi Ahmadian. You have my deepest gratitude and I hope that one day I become as good to my students as you have been to me.

My sincere thanks goes to Dr. Brian Vick, Dr. Norman Dowling, Dr. Dong Ha, Dr. Steve Southward, and Dr. John Kennedy for serving on my doctoral advisory committee. Your comments and constructive criticism of my research help me focus and enrich my ideas.

I would like to acknowledge Mr. Carvel Holton for his generous support and fruitful discussions that helped me improve my knowledge. I would also like to thank my friends, Masood Taheri and Sajjad Meymand, for their assistance and support throughout the project.

I acknowledge and appreciate the support provided by Norfolk Southern's Research and Tests Department. In particular, I am thankful to Mr. Brad Kerchof and Mr. Kevin Conn for their tremendous support during rail inspection testing.

I am also grateful to my labmates at CVeSS for their various forms of support during my graduate study and for all the fun we have had in the last three years. I also thank my wonderful friends in Blacksburg- their support and care helped me overcome setbacks and stay focused on my graduate study.

Most importantly, none of this would have been possible without the love and patience of my lovely family: my parents, wife, and children. Thank you!

Contents

CHAPTER 1 INTRODUCTION 1

1.1 MOTIVATION 1

1.2 OBJECTIVES 2

1.3 APPROACH 3

1.4 CONTRIBUTIONS 4

1.5 OUTLINE 5

CHAPTER 2 LITERATURE REVIEW AND BACKGROUND 6

2.1 TRACK GEOMETRY IRREGULARITIES 6

2.1.1 PROFILE 6

2.1.2 CROSS LEVEL 7

2.1.3 ALIGNMENT 8

2.1.4 GAGE 8

2.2 TRACK VIBRATION 9

2.3 RAIL AND WHEEL INTERACTION 10

2.4 TRACK LUBRICATION 11

2.4.1 EFFECT OF LUBRICATION 12

2.4.2 METHODS OF LUBRICATION 13

2.4.3 RAIL AND LUBRICATION INSPECTION 13

2.5 LASER AND LIGHT 15

2.6 LAMBERTIAN REFLECTANCE 15

2.7 LAMBERT'S COSINE LAW 16

2.8 SPECULAR AND DIFFUSE REFLECTION 17

2.9 GLOSS AND ABSORPTION 18

2.10 SIGNAL PROCESSING 19

CHAPTER 3 EXPERIMENTAL SETUPS 22

3.1 LAB TRACK SYSTEM SETUP 22

3.2 FIELD TRACK SYSTEM SETUP 24

CHAPTER 4 LAB TRACK SYSTEM RESULTS 28

4.1 LUBRICATION DETECTION 28

4.1.1 LUBRICANT A 31

4.1.2 LUBRICANT B 32

4.1.3 LUBRICANT C 34

CHAPTER 5 FIELD TRACK RESULTS 36

5.1 LUBRICATION DETECTION 36

5.1.1 LUBRICANT A 38

5.1.2 LUBRICANT B 38

5.1.3 LUBRICANT C 40

CHAPTER 6 REVENUE SERVICE TRACK TESTING 42

6.1 PLAN AND PREPARATION 42

6.2 SETUP AND NEW CART 45

6.3 RESULTS AND DATA ANALYSIS 47

CHAPTER 7 SYSTEM PARAMETERS EFFECT 57

7.1 LAYER THICKNESS 57

7.1.1 LUBRICANT A 57

7.1.2 LUBRICANTS B AND C 59

7.2 VIBRATION AND MOTION 60

7.3 AMBIENT LUMINANCE 62

7.4 ANGLE OF INCIDENCE 64

CHAPTER 8 LUBRICATION QUANTIFICATION 67

8.1 BOOLEAN ASSIGNMENT 67

8.2 LUBRICATION INDEX 70

CHAPTER 9 CONCLUSIONS AND FUTURE WORK 73

9.1 SUMMARY AND CONCLUSIONS 73

9.2 FUTURE WORK 75

REFERENCES 76

APPENDIX A LUBRICANTS SPECIFICATION 78

A.1 LUBRICANT A 78
A.2 LUBRICANT B 78
A.3 LUBRICANT C 79

APPENDIX B LASER SPECIFICATIONS 80

B.1 SENSOR HEAD SPECIFICATION: LV-NH32 80
B.2 SENSOR AMPLIFIER SPECIFICATION: LV-N11MN 81
B.3 MONITOR OUTPUT TYPE INPUT/OUTPUT CIRCUIT DIAGRAM 82

List of Figures

FIGURE 2-1 TRACK PROFILE VARIATION 7
FIGURE 2-2 TRACK ELEVATION VARIATIONS (CROSS LEVEL) 7
FIGURE 2-3 TRACK ALIGNMENT DEVIATION 8
FIGURE 2-4 TRACK GAGE VARIATION 9
FIGURE 2-5 FORCES ACTING ON TRAIN WHEELSET 10
FIGURE 2-6 RADIANT INTENSITY IN NORMAL AND OFF-NORMAL DIRECTIONS 16
FIGURE 2-7 DIFFUSE AND SPECULAR REFLECTION FROM A SURFACE REFLECTING AN INCIDENT LIGHT 18
FIGURE 2-8 FILTER DESIGN ILLUSTRATION: LOW-PASS FILTER, HIGH-PASS FILTER, AND BAND-PASS FILTER 20
FIGURE 2-9 A FUNCTION IN TIME AND FREQUENCY DOMAIN 21
FIGURE 3-1 YARD CURVED SECTION OF TRACK 24
FIGURE 3-2 LASER HEAD MOUNTED 3 FT. HIGH WITH RESPECT TO RAIL 25
FIGURE 3-3 SCANNING CART WITH LASER PROCESSING SYSTEM ON-BOARD 25
FIGURE 3-4 RED REFLECTIVE TAPE ACTS AS RAIL SECTIONS MARKERS 26
FIGURE 3-5 APPLYING TOR LUBRICANTS USING SMALL ROLLER 26
FIGURE 3-6 A THIN LAYER OF LUBRICANT C ON TOP OF RAIL 27
FIGURE 4-1 LAB TRACK UNLUBRICATED RAIL SPECULAR REFLECTION VOLTAGE 29
FIGURE 4-2 LAB TRACK UNLUBRICATED RAIL SPECULAR REFLECTION FFT 29
FIGURE 4-3 LAB TRACK UNLUBRICATED RAIL SPECULAR REFLECTION FFT MAGNIFIED 30
FIGURE 4-4 LAB TRACK UNLUBRICATED RAIL SPECULAR REFLECTION MEAN VALUE WITH HIGH-PASS FILTER 30
FIGURE 4-5 LUBRICANT A SPECULAR REFLECTION COMPARED TO LAB TRACK UNLUBRICATED RAIL 31
FIGURE 4-6 LUBRICANT A SPECULAR REFLECTION MEAN VALUE WITH HIGH-PASS FILTER COMPARED TO LAB TRACK UNLUBRICATED RAIL 32
FIGURE 4-7 LUBRICANT B SPECULAR REFLECTION COMPARED TO LAB TRACK UNLUBRICATED RAIL 33
FIGURE 4-8 LUBRICANT B SPECULAR REFLECTION MEAN VALUE WITH HIGH-PASS FILTER COMPARED TO LAB TRACK UNLUBRICATED RAIL 34
FIGURE 4-9 LUBRICANT C SPECULAR REFLECTION COMPARED TO LAB TRACK UNLUBRICATED RAIL 35
FIGURE 4-10 LUBRICANT C SPECULAR REFLECTION MEAN VALUE WITH HIGH-PASS FILTER COMPARED TO LAB TRACK UNLUBRICATED RAIL 35
FIGURE 5-1 SPECULAR REFLECTION OF YARD RAIL IN UNLUBRICATED CONDITION 37
FIGURE 5-2 YARD UNLUBRICATED RAIL SPECULAR REFLECTION FFT 37

FIGURE 5-3 LUBRICANT A SPECULAR REFLECTION COMPARED TO YARD UNLUBRICATED RAIL 38
FIGURE 5-4 LUBRICANT B SPECULAR REFLECTION COMPARED TO YARD UNLUBRICATED RAIL 39
FIGURE 5-5 DIFFERENT LAYER THICKNESSES OF LUBRICANT B COMPARED TO UNLUBRICATED RAIL SPECULAR REFLECTION 40
FIGURE 5-6 LUBRICANT C SPECULAR REFLECTION COMPARED TO YARD UNLUBRICATED RAIL 41
FIGURE 6-1 TEST SITE MAP, LOCATION, TRAIN DIRECTION, AND PICTURES OF TEST TRACK SECTIONS ..43
FIGURE 6-2 WAYSIDE LUBRICATOR STATION NEAR TEST RAIL 44
FIGURE 6-3 CLOSE-UP PICTURE OF THE LUBRICATOR PUMPING LUBRICANT ON TOP OF RAIL 44
FIGURE 6-4 MODIFIED CART EQUIPPED WITH LASER SENSOR, ENCODER, AND DATA ACQUISITION SYSTEM 45
FIGURE 6-5 VELOCITY OF A MANUALLY-PUSHED CART ON AN UNLUBRICATED TANGENT TRACK 46
FIGURE 6-6 VELOCITY OF A MANUALLY-PUSHED CART ON A LUBRICATED CURVED TRACK 47
FIGURE 6-7 LASER SENSOR OUTPUT OF THE SOUTHBOUND TRACK TEST WITH DIFFERENT LUBRICATION AND LUMINANCE CONDITIONS 48
FIGURE 6-8 LASER SENSOR OUTPUT OF AN UNLUBRICATED TANGENT TRACK IN THE SOUTHBOUND TEST (HIGH RAIL) 48
FIGURE 6-9 LASER SENSOR OUTPUT OF A LUBRICATED TANGENT TRACK IN THE SOUTHBOUND TEST (HIGH RAIL) 49
FIGURE 6-10 SECTION OF THE RAIL AFTER THE LUBRICATOR SHOWING DISCRETE PATCHES OF LUBRICANT 50
FIGURE 6-11 LASER SENSOR OUTPUT OF A LUBRICATED CURVED TRACK IN THE SOUTHBOUND TEST (HIGH RAIL) 50
FIGURE 6-12 LASER SENSOR OUTPUT OF AN UNLUBRICATED TANGENT TRACK IN THE NORTHBOUND TEST (LOW RAIL) 52
FIGURE 6-13 LASER SENSOR OUTPUT OF A LUBRICATED TANGENT TRACK IN THE NORTHBOUND TEST (LOW RAIL) 52
FIGURE 6-14 LASER SENSOR OUTPUT OF A LUBRICATED CURVED TRACK IN THE NORTHBOUND TEST (LOW RAIL) 53
FIGURE 6-15 LUBRICITY INDEX FOR SOUTHBOUND AND NORTHBOUND TEST SECTIONS 56
FIGURE 7-1 SPECULAR REFLECTION OF DIFFERENT LAYER THICKNESSES OF LUBRICANT A COMPARED TO UNLUBRICATED RAIL (LAB TRACK) 58
FIGURE 7-2 SPECULAR REFLECTIONS OF DIFFERENT THICKNESS LAYERS OF LUBRICANT B 59
FIGURE 7-3 SPECULAR REFLECTIONS OF DIFFERENT THICKNESS LAYERS OF LUBRICANT C 60
FIGURE 7-4 VIBRATION-SIMULATING MACHINE WITH INSTALLED LASER SYSTEM 61
FIGURE 7-5 EFFECT OF LATERAL VIBRATION ON LASER SENSOR OUTPUT 62
FIGURE 7-6 LASER SENSOR OUTPUT OF TWO DIFFERENT LIGHTING CONDITIONS FOR THE SAME SPOT 63
FIGURE 7-7 SENSOR HEAD SETUP FOR DIFFUSE REFLECTION OF AN UNEVEN SURFACE 64

FIGURE 7-8 SENSOR HEAD WITH INCORRECT SETUP FOR SPECULAR REFLECTION OF A SHINY SURFACE 65
FIGURE 7-9 SENSOR HEAD ADJUSTMENTS FOR SPECULAR REFLECTIONS OF A SHINY SURFACE 65
FIGURE 8-1 UNLUBRICATED RAIL SPECULAR REFLECTION WITH MEAN AND STANDARD DEVIATION COMPARED TO LUBRICANT A 68
FIGURE 8-2 UNLUBRICATED RAIL SPECULAR REFLECTION WITH MEAN AND STANDARD DEVIATION COMPARED TO MINIMUM AMOUNT OF LUBRICANT A 69
FIGURE 8-3 UNLUBRICATED RAIL SPECULAR REFLECTION WITH MEAN AND STANDARD DEVIATION COMPARED TO LUBRICANT C 70
FIGURE 8-4 MEAN AND STANDARD DEVIATIONS IN NORMAL DISTRIBUTION 71
FIGURE 8-5 COMPARISON BETWEEN LUBRICANT C AND UNLUBRICATED RAIL MEAN VALUES 71
FIGURE B–1 MONITOR OUTPUT CIRCUIT DIAGRAM 82

List of Tables

TABLE 2-1 LUBRICATION CHART SUMMARY 14
TABLE 6-1 TRACK SECTIONS IN SOUTHBOUND AND NORTHBOUND TESTS 44
TABLE 6-2 AVERAGE VALUES OF THE LASER SENSOR OUTPUTS IN THE SOUTHBOUND TEST FOR EACH SECTION 51
TABLE 6-3 AVERAGE VALUES OF THE LASER SENSOR OUTPUTS IN THE NORTHBOUND TEST FOR EACH SECTION 53
TABLE 6-4 SHIFTED AVERAGE VALUES OF THE LASER SENSOR OUTPUTS FOR SOUTHBOUND AND NORTHBOUND TEST SECTIONS 55
TABLE A–1 LUBRICANT A SPECIFICATION 78
TABLE A–2 LUBRICANT B SPECIFICATION 78
TABLE A–3 LUBRICANT C SPECIFICATION 79
TABLE B–1 SENSOR HEAD SPECIFICATION (LV-NH32) 80
TABLE B–2 SENSOR AMPLIFIER SPECIFICATION (LV-N11MN) 81

Nomenclature

$\mathrm{s(x,y)}$	Creepage at any point in the contact zone
$\mathrm{Q(x,y)}$	Distribution of surface traction
$\mathrm{K_s}$	Wear coefficient depends on material properties and slip
$\mathrm{K_p}$	Wear coefficient depends on material properties and contact pressure
ℓ	Lubrication Index
ℓ_i	Lubrication Index of i^{th} rail segment
x_i	Length of the i^{th} segment
$\overline{\ell}$	Overall Lubrication Index
$\overline{D}$	Mean reflection values of unlubricated rail
$\overline{L}$	Mean reflection values of lubricated rail
σ_D	Standard deviation of unlubricated rail reflection values
I	Luminous intensity
I_{MAX}	Maximum luminous intensity
R_s	Specular reflectance
θ	Angle of incidence
I_r	Reflected beam intensity
m	Refractive index
f_c	Cutoff frequency
$\mathcal{L}$	Lubricity Index
R_D	Unlubricated rail reflection
R_x	Reflection at point x
v_x	Creepage in longitudinal direction
$\boldsymbol{c_w}$	Wheel circumferential velocity vector
$\boldsymbol{c_r}$	Rail circumferential velocity vector

Chapter 1
Introduction

1.1 Motivation

With increased attention to the benefits of rail lubrication, the railroad industry has developed an increased interest in more accurately assessing the relationships between top-of-rail lubrication and its effect on rail wear, contact fatigue, curving resistance, fuel efficiency, and other operational elements. As an example, recent test data have shown that effective lubrication can extend the wear life of standard high-carbon rail by factors of three or more in moderately and heavily curved tracks.

One of the key elements related to maintenance of the rail is determining the optimum, or near optimum, amount of rail lubricant for attaining the benefits of Top of Rail (TOR) lubrication, without wasting too much lubricant. Establishing a quantifiable relationship between the amount of lubricant and the resulting benefits starts with the ability to directly and accurately measure the state of rail lubrication upon the application of TOR friction modifiers.

Several factors have motivated the study described in this dissertation. Specifically, they are related to operational cost and efficiency for railroad operation, maintenance, and inspection quality and frequency, as will be detailed in this study.

Lubrication systems use a consumable and ecologically safe lubricant on top of both rails after the last locomotive axle has passed the lubricant applicator. The rate of application of the lubricant is computed in real time by an on-board computer, and is based on instantaneous train and track parameters, including train speed, train tonnage, degree of track curvature, ambient temperature, brake application, direction of travel, and locomotive position and orientation.

Railroad track lubricity conditions are regularly inspected by the track administrators. The collected TOR lubricant data are then evaluated and used for track and maintenance planning, lubricant effectiveness evaluation, and train speed settings. Although visual TOR inspection is a common practice, it is purely empirical and highly dependent on the skills and experience of the track engineer. The inspection is susceptible to large variation, mainly due to the skill level of the inspectors. Therefore, it is beneficial for the inspectors to be equipped with a reliable TOR lubricant detection instrument.

1.2 Objectives

The primary objectives of this study are to:

1. Assess the effectiveness and utility of laser-based measurement systems for detecting the state of TOR friction modifiers for railroad applications,
2. Develop a practical and portable system that can be used for accurately and repeatedly measuring TOR lubricity in conditions commonly existing in revenue service track,
3. Conduct laboratory and field tests that will prove the merits of the measurement system and develop a quantifiable measure that can be used by railroad practitioners, and
4. Provide recommendations for other efforts that can extend the findings of this research.

1.3 Approach

The following approach is used to address the issues presented in this study:

- Processing algorithms are developed to separate the effect of surface irregularities from lubricant specular reflections.
- A laser sensor system, including a remotely moving cart, available at Railway Technologies Laboratory (RTL) of Virginia Polytechnic Institute and State University (VT), is mounted to a yard rail track.
- A laser sensor with an amplifier is used to detect and measure specular and diffuse reflection.
- The system is set up and installed on revenue service track in order to study any differences with lab experiments.
- A 40-ft rail panel at Railway Technologies Laboratory (RTL) of Virginia Polytechnic Institute and State University (VT) is used for lubrication detection tests. Red reflective markers are placed at 1-ft intervals to mark the test section into separate sub-sections.
- A 250-ft curved section of track near Roanoke, Virginia is measured manually to obtain a ground truth test section for system calibration. Red reflective markers are used at 50-ft intervals along the test section to optically mark the track into separate regions, each with a unique lubricant or lubrication condition.
- The data gathered during the tests are processed using different signal processing techniques to obtain the measurement of interest: specular reflection. Comparisons are made between unlubricated and lubricated rail, with different amounts of lubrication, to establish the relative differences.
- The results of the tests are used to provide an evaluation of the laser system's functionality for rail applications.
- The repeatability and universality of the measurements are examined by analyzing the data for different sections of the track.

- Different approaches to analyzing the measurement system's output are presented quantify TOR lubricity, including the development of a Lubrication Index for numerically assessing the condition of the rail.
- The effect of track environment, such as rain, light, and surface roughness, on the accuracy of the measurements is determined.

1.4 Contributions

The contributions of the research presented in this study to the railroad industry are:

- Development of an innovative system for railroad TOR lubrication monitoring,
- Providing accurate records of rail lubrication monitoring parameters such as lubrication percentage and layer thickness,
- Extension of laser technology applicability and further development of lubricant monitoring for demanding railroad environments,
- Introducing a method of railroad lubricant monitoring that is versatile in physical configuration, and allows for focusing on a particular target parameter if desired,
- Establishing a lubrication index to evaluate the overall track lubrication condition, and
- Development of a track TOR lubricant maintenance model that predicts the best time for track inspection.

1.5 Outline

The information in the following chapters of this dissertation is organized according to the following outline:

- Chapter 1 introduces the study and provides the objectives, approach, potential contributions, and an outline of the dissertation.
- Chapter 2 provides the technical background and literature review for the study. Track geometry parameters, track vibration, rail and wheel wear, track lubrication, and specular and diffuse reflection are also presented.
- Chapter 3 details the laser sensor system installation for laboratory assessment on a lab track panel, in preparation for field testing on a longer section of track in a railroad yard.
- Chapter 4 discusses the results of lubrication monitoring for different types of lubricants using laser technology on lab track panel.
- Chapter 5 discusses the results of using the laser measurement system to evaluate the effectiveness of the system in detecting various amounts of TOR lubricant on a yard track, with different types of rail lubricants manually applied at varying amounts to the rail.
- Chapter 6 discusses the results of using the laser measurement system to evaluate the effectiveness of the system in detecting TOR lubricant on a revenue service track, using wayside lubricators and passing trains.
- Chapter 7 presents the effects of other system parameters, such as lighting and layer thickness on the results and the effectiveness of lubrication detection and monitoring.
- Chapter 8 presents various approaches and models to quantify lubricant monitoring results based on specular reflection measurements made by the laser measurement system.
- Chapter 9 provides the final conclusions and presents recommendations for future studies in continuing this effort.

Chapter 2
Literature Review and Background

This chapter provides the technical background essential for understanding the principles underlying the research performed in this study. An overview of track geometry characteristics is presented, along with a brief introduction of wheel and rail wear. Next, a background of rail track lubrication is presented. The chapter is concluded with introducing laser technology as a reliable tool for rail lubrication detection and measurements.

2.1 Track Geometry Irregularities

The nominal centerline is the ideal path of the track where rails are laid and installed. However, there will always be small deviations from the nominal path. Left and right surface profiles and cross level describe the vertical irregularities, where left and right alignment and gage describe the irregularities that occur laterally. Extreme track geometry variations can lead to large wheel and axle forces, resulting in derailment, excessive body acceleration, and damage to the track structure. In the following sections, these irregularities are introduced and briefly discussed.

2.1.1 Profile

Track profile is defined as the vertical deviation of the midpoint of the two rails from the nominal elevation, as shown in Figure 2-1. A positive profile variation corresponds to an upward vertical deviation of the track, and a negative variation refers to a downward vertical deviation of the track.

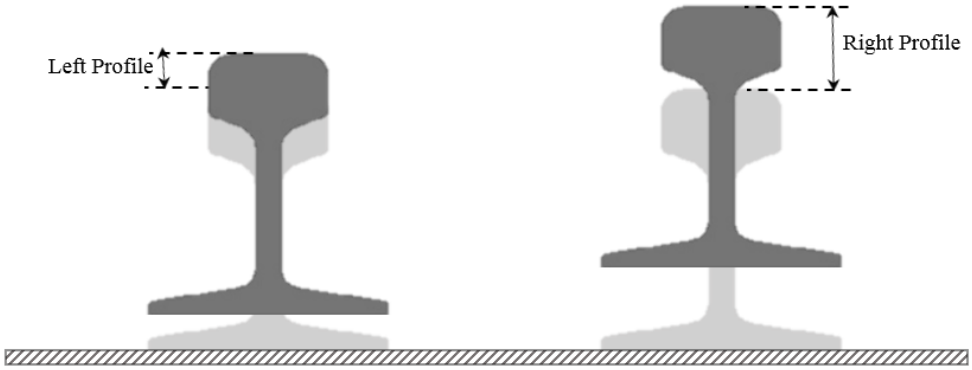

Figure 2-1 Track profile variation

2.1.2 Cross Level

Cross level is defined as the vertical difference between the left and right rail from the nominal distance, as shown in Figure 2-2. The anticipated distance refers to the amount of superelevation. If superelevation equals zero, then cross level is the difference between the elevations of the left and right rail. A positive cross level represents a situation when the left rail is placed above the right rail, while a negative cross level refers to a case when the left rail is laid below the right rail.

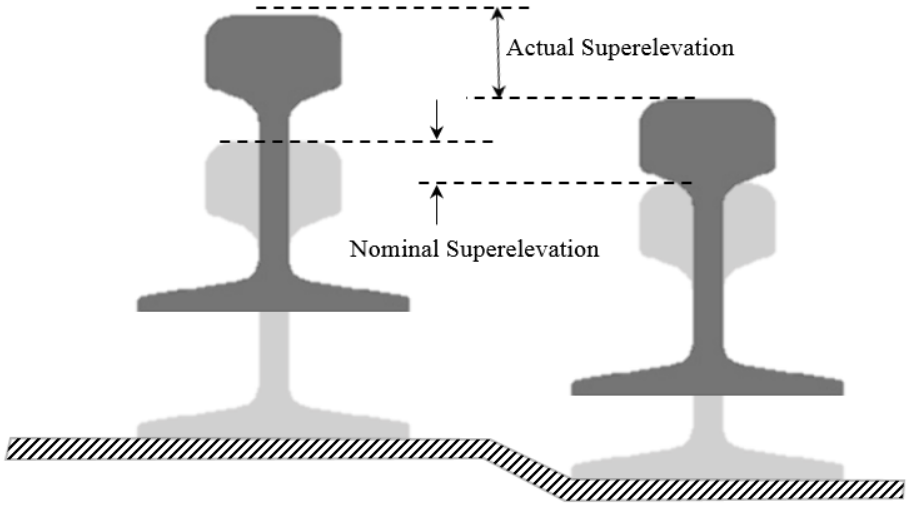

Figure 2-2 Track elevation variations (Cross level)

2.1.3 Alignment

Track alignment is the variation in the lateral positions of the left and right rails from a mean trajectory over a specific length of the track. Alignment deviations for the left and right tracks are shown in Figure 2-3. Alignment can be measured manually using chord-based approaches, where the lateral offset of the rail from the center of a string stretched between two ends touching the rail side is obtained at multiple locations [1]. A positive deviation in the alignment denotes a lateral deviation of the track to the left, while a negative deviation in the alignment corresponds to a lateral deviation of the track to the right.

Figure 2-3 Track alignment deviation

2.1.4 Gage

Gage is defined as the distance between the two rails measured 5/8 inches below the top of each rail. Gauge can be measured manually using a gauge measuring stick [1]. Gage can also be defined as the lateral deviation of the track from its nominal gage, which is 56.5 inches on U.S. railroads, as shown in Figure 2-4. When discussing the track geometry, gage variation is commonly used. Positive gage variation represents the widening of the gage, while a negative variation corresponds to a narrowing of the gage.

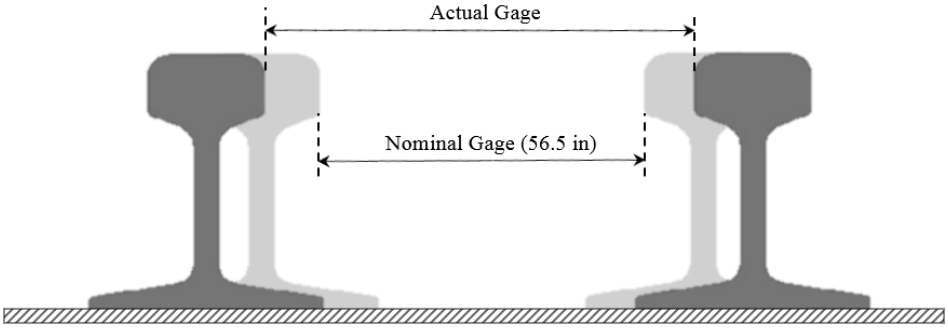

Figure 2-4 Track gage variation

2.2 Track Vibration

Track-induced noise and vibrations are irritating and disruptive, especially for people living alongside the railway lines. Therefore, rail administrators are expected to keep this disturbance below certain destructive levels. Track vibrations are mainly caused by large fluctuating forces between rails and wheels when a train travels on the rails. The fluctuations in forces are originated from wheel roughness and/or track irregularities. Track vibrations mostly occur at lower frequencies below 50 Hz [2].

The severity and magnitude of the transmitted track-induced vibrations are determined by studies at the foundation of buildings near the track lines using accelerometers [3]. Vibration measurement is not, however, limited to stationary in-site acceleration measurements. Continuous vibration monitoring is possible using Light Detection and Ranging (LIDAR) technology [4, 5].

2.3 Rail and Wheel Interaction

Train dynamics modeling, especially the interaction between wheels and rails, plays an important role in keeping the wheels on the track and avoiding derailment. A conical design for train wheels is used to assure that the wheels are centered on the rail. With the existence of friction, the rotational speed of the wheels becomes smaller than the translational speed, which introduces creepage. In normal situations, there is one point of contact per wheel that will be moved due to the relative lateral, vertical, and yaw movement of the wheel set with respect to the track centerline. In other cases, multiple contact points can be present.

Figure 2-5 shows longitudinal (F_x) and lateral (F_y) forces acting on the train wheelset. These forces cause a steering moment that helps the train travel through a curve. Higher lubrication causes lower friction forces, which leads to wheels spinning in place on the low rail. This helps create a higher moment in the required curve direction. On the other hand, and with improper friction management, the difference in longitudinal forces can be minimal, which requires higher lateral forces to have the same resultant steering moment. This increase in lateral force values will have a negative effect on the wear of the wheels and rails.

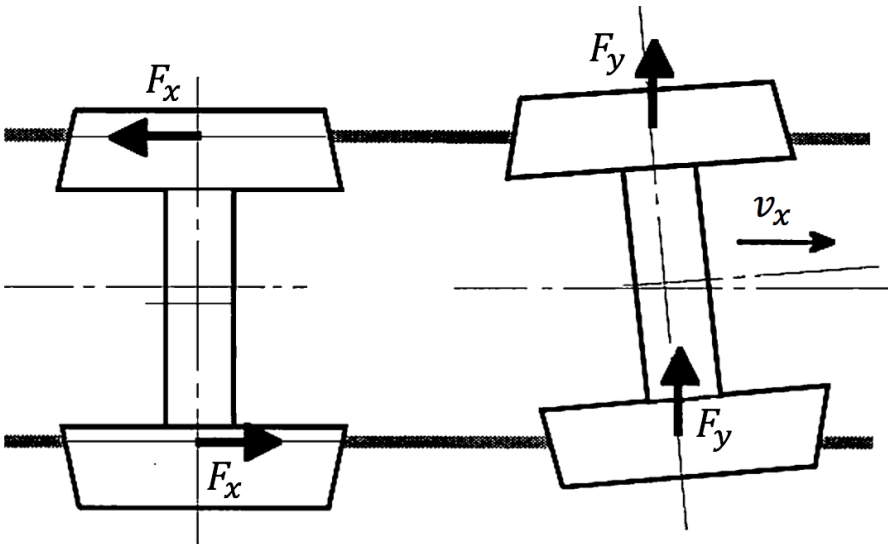

Figure 2-5 Forces acting on train wheelset

The profile change of rails in curves makes a large contribution to track maintenance costs. The effect of profile change on wheels can also be significant, especially on a curved track. Damage mechanisms such as wear and plastic deformation are the main contributors to profile change. Wear is usually modeled as an energy dissipation process [6], such that the volume of wear is related to the frictional energy by some wear constant:

$$\text{Wear} = K_{s,p} \iint_{\text{contact area}} s(x,y)Q(x,y)\Delta x\Delta y \tag{2-1}$$

where $s(x,y)$ is the creepage at any point in the contact zone, $Q(x,y)$ is the distribution of surface traction, and K is the wear coefficient that depends not only on material properties, but also on slip and contact pressure, thus the subscripts s and p, respectively. Any quantitative analysis demands that K be calculated under well-controlled circumstances for the contact being modeled. Regardless, it can be said that reducing the traction (usually, via friction control) and creepage (through improved profiles and bogies) are the keys to reducing wheel/rail wear.

An understanding of the tribology of the wheel/rail system is essential if wheel/rail life is to be extended. This system is complex, and its behavior depends on interactions between the materials (wheel, rail, and any third body introduced, such as lubricant/debris mixtures) and the stress-temperature environment (which is a function of vehicle weight, vehicle/track interaction, wheel/rail profiles, wheel/rail adhesion, and speed).

2.4 Track Lubrication

The trackside lubrication system applies a consumable, and environmentally safe, lubricant on top of both rails after the last locomotive axle has passed the applicator location. The amount of lubricant dispensed on the rails is computer-controlled so that the lubricant is consumed by the time the entire train has passed. The rate of application of the lubricant is computed in real time by an on-board computer [7], and is based on the following instantaneous train and track

parameters: train speed, train tonnage, degree of track curvature, ambient temperature, break application, direction of travel, and locomotive position and orientation.

2.4.1 Effect of Lubrication

Based on test data [8] that show a 32% savings in fuel consumption along the lubricated test track, considerable energy savings would result from trackside lubrication. The fuel reduction values were supported by measured reductions in lateral wheel/rail forces on the Facility for Accelerated Service Testing (FAST) loop in both tangent and curved sections. It was noticed [9] that 30% fuel savings were achieved in running 100-ton capacity cars at a constant speed of 40 miles per hour in a fully-lubricated FAST loop (gauge face and rail head covered by a film of lubricant) with respect to unlubricated conditions. Samuels and Tharp [10] reported a 25-30% savings for unit coal train operations on one specific route with a large number of sharp curves. Dahlman and Stehly [11] carried out tests on mainly level, tangent track and produced average savings of about 5%, which shows that lubrication has greater effect on curves.

Many railroads installed locomotive lubricators to supplement existing trackside devices on the strength of such results. Recently, some railroads have begun to determine the net savings, taking into account the cost of installing and maintaining locomotive lubricators. The perception is that they are no more reliable than trackside lubricators. The recent enthusiasm for improved lubrication is tempered, then, by the frustration of equipment reliability, echoing the experience of a previous era [12, 13]. In North America, there is the added complication of variation in performance under different climatic conditions. Furthermore, there are many lubricants available with few comparative data to guide purchasers.

Lateral forces produced on the rails in curves are the result of track and truck performance. When excessive, these forces can lead to derailment by rail rollover or wheel climb, and they are a contributing cause of both track damage and a high cost of track maintenance. Lateral forces were reduced significantly by using top-of-rail lubrication [14]. Top-of-rail (TOR) lubrication is capable of considerably reducing the amount of energy required to move a train. Top-of-rail lubrication also resulted in significant reduction of lateral loading on the rail.

2.4.2 Methods of Lubrication

There are two commonly known methods of rail lubrication: vehicular-mounted lubricators (devices on moving vehicles), and wayside lubricators (devices that are permanently located at fixed points in the track).

For the first method, vehicular-mounted lubrication systems, three distinct types of vehicle-mounted lubrication systems have emerged: hi-rail vehicle systems, locomotive-mounted systems, and a dedicated lubricator car. All three have been built and tested, including a recent series of evaluation tests at FAST, where they have been compared with wayside lubricator systems.

The second method, wayside lubricators, is the traditional approach that has been used by railroads for many years. Most wayside lubricators employ some form of mechanical applicator system to apply a predetermined amount of lubricant to each passing wheel-flange. As a result, every wheel of every train carries a small amount of lubricant applied to its flange. The wheel flange then carries the lubricant along and applies it to the rail for some limited distance.

2.4.3 Rail and Lubrication Inspection

The accuracy and efficiency of the inspecting equipment determine the effectiveness of rail inspection [15], in addition to the the skills and experience of the inspectors. Errors and mistakes mainly depend on the limitation of inspection equipment and on the skill level of rail inspectors. These errors in inspection are important issues, and their reduction is a big challenge. Table 2-1 shows a brief description guide to determine whether the gauge face is adequately lubricated [16].

Table 2-1 Lubrication chart summary

Classification	Coefficient of friction	Description
Dry	0.35 to 0.57	No grease on wear face
Poor	0.30 to 0.35	Lubricant on 10 to 40 percent of the wear face
Acceptable	0.25 to 0.30	Lubricant on 40 to 60 percent of the wear face
Average	0.20 to 0.25	Lubricant on 60 to 90 percent of the wear face
Good	0.15 to 0.20	Lubricant on 100 percent of the wear face
Too much	<0.15	Gauge face and rail head covered by a film of lubricant

Weather conditions have an effect on the inspection process. Inspection of the rail becomes a difficult and costly matter in winter, especially in cold countries. Management of rail traffic during inspection is another factor. The busier the rail routes become, the more difficult it is to stop train traffic and perform rail inspection and maintenance. In these routes, rail inspection is done during the night, which forces the responsible authorities to pay workers and inspectors more for working during nighttime. It is a challenge to effectively carry out inspection and maintenance procedures with optimal rail inspection and maintenance cost, while at the same time causing minimal traffic interruption.

To reduce the cost as well as the derailment risk and rail/wheel damage, optimum frequency of lubrication requires a detailed model: “Effective lubrication can only be enforced if adequate monitoring methods are available,” [17]. Thus, the sensors to actuate the lubricators should also be sensitive enough to optimize lubrication frequency.

2.5 Laser and Light

A laser, an acronym for Light Amplification by Stimulated Emission for Radiation, is created [18] when electrons in atoms absorb energy from an electrical current and become excited, and then move from a lower-energy orbit to a higher one around the atom's nucleus. The electrons emit photons when they return to their normal state.

There are unique properties of a laser that make it different from normal light:

- Directionality: conventional light sources emit light in all directions, while lasers generate a very tight beam that spreads slightly with distance.
- Monochromaticity: normal light sources emit light that consists of a vast range of wavelengths. A laser, on the other hand, contains only one or a narrow range of wavelengths.
- Coherence: In contrast with normal light, all parts of a laser's electromagnetic waves are in phase.

If designed carefully, purity of light emitted by the laser can be improved more so than any other source of light, which makes it a useful source for spectroscopy [19], which is the study of the interaction between matter and electromagnetic radiation.

2.6 Lambertian Reflectance

The effectiveness in reflecting radiant energy of a material surface is called reflectance; it is the fraction of incident electromagnetic power (e.g. light) that is reflected at an interface [20]. Lambertian reflectance is the property that describes a diffusely reflecting surface (i.e. an ideal matte). For a surface to be a Lambertian surface, the apparent brightness of it has to be the same regardless of the observer's angle of view. This means that a Lambertian surface's luminance is isotropic and follows Lambert's cosine law, which will be explained later.

Rough surfaces, like wood, generally demonstrate Lambertian reflectance. Reflection from polished surfaces is often accompanied by specular reflection, which differs in surface luminance according to the observer's angle of view; it is highest when the observer is at the perfect reflection direction (according to the law of reflection).

2.7 Lambert's Cosine Law

Luminous intensity is a measure of the wavelength-weighted power emitted by a light source in a particular direction per unit solid angle. According to Lambert's cosine law, the luminous intensity (I) observed from an ideal, diffusely reflecting surface is directly proportional to the cosine of the angle θ between the surface normal and the direction of the incident light, as illustrated in Figure 2-6.

$$I = I_{MAX} \cos\theta \tag{2-2}$$

where I is radiant or luminous intensity in candelas (cd), and θ is the angle measured between the surface normal and the direction of the incident light.

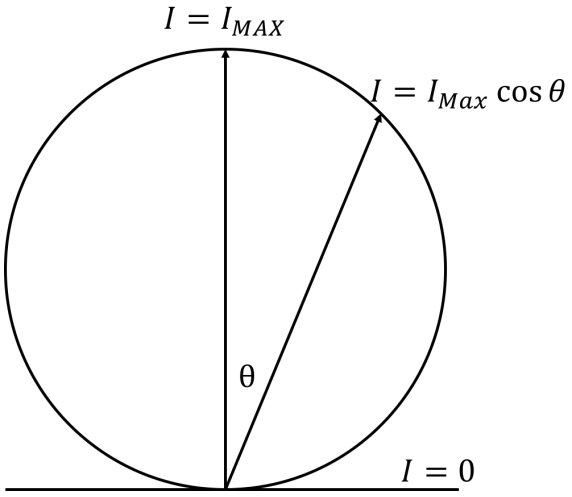

Figure 2-6 Radiant intensity in normal and off-normal directions

2.8 Specular and Diffuse Reflection

According to the law of reflection, light reflects off surfaces in a predictable manner. The light ray always reflects in such a way that the angle of incidence is equal to the angle of reflection. This predictability concerning the reflection of light is applicable to the reflection of light off of level (horizontal) surfaces, vertical surfaces, angled surfaces, and even curved surfaces. As long as the normal (perpendicular line to the surface) can be drawn at the point of incidence, the angle of incidence can be measured and the direction of the reflected ray can be determined.

Reflection of smooth surfaces, such as mirrors or a calm body of water, leads to a type of reflection known as specular reflection. Reflection of rough surfaces, such as clothing, paper, and the asphalt roadway, leads to a type of reflection known as diffuse reflection. A tremendous impact upon the subsequent reflection of a beam of light depends on whether the surface is microscopically rough or smooth.

Figure 2-7 shows how diffuse and specular reflections of light from a surface differ such that an incident ray is reflected at many angles in the case of diffuse reflection, and in one angle as in the case of specular reflection [21]. Almost all materials can give specular reflection if their surface can be polished to eliminate irregularities comparable with light wavelength (a fraction of a micrometer).

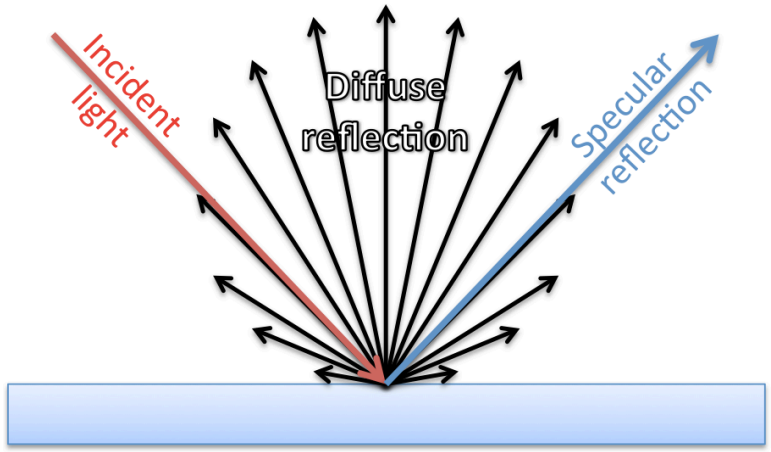

Figure 2-7 Diffuse and specular reflection from a surface reflecting an incident light

Diffuse reflection from white materials can be highly efficient in giving back all the light that these materials receive, due to the summing up of the many subsurface reflections. Furthermore, diffusion substantially affects the color of objects because it determines the average path of light in the material, and hence, to which extent the various wavelengths are absorbed [22]. This property of colored objects will be of significant importance when detecting lubrication.

2.9 Gloss and Absorption

Light interacts with an object in different ways: it can be absorbed, transmitted, scattered, and reflected. Reflectance and absorption are important in this study because they have surface properties that are associated with them which allows for the quantification of how light interacts with an illuminated object.

How well a surface reflects light in a specular direction is defined as an optical property called gloss. Gloss is affected by material refractive index, angle of incident light, and surface topography, and is quantified [23] by the Fresnel formula (2-3(2-4) which measures how reflective (R_s) the surface is. It depends on light intensity (I_0), angle of incidence (θ), the reflected beam intensity in the specular direction (I_r), and material refractive index (m).

$$R_s = \frac{I_r}{I_0} \tag{2-3}$$

$$R_s = \frac{1}{2}\left[\left(\frac{\cos\theta - \sqrt{m^2 - \sin^2\theta}}{\cos\theta + \sqrt{m^2 - \sin^2\theta}}\right)^2 + \left(\frac{m^2\cos\theta - \sqrt{m^2 - \sin^2\theta}}{\mathrm{m}^2\cos\theta + \sqrt{m^2 - \sin^2\theta}}\right)^2\right] \tag{2-4}$$

Since material refractive index affects how reflective the surface is, non-metallic materials absorb or diffuse more light at a greater illumination angle compared to metals. Metals produce higher amounts of reflected light at any angle.

Absorption is a property that defines how the material takes up the energy of a photon [24], and is quantified by determining how much of the incident light is absorbed by an object. Commonly, the absorption of light does not depend on its intensity. Accurate measurements of the absorbance at different wavelengths allow the identification of a substance.

2.10 Signal Processing

Filters are often named according to the frequency range that they allow to pass. The rest are blocked. Three of the most commonly used filters are described [25] and illustrated in Figure 2-8:

- **High-pass Filter**

  A high-pass filter is usually an electronic filter that allows signals with a frequency range higher than a certain specified frequency, and blocks signals with lower frequency range. This specified frequency is called cutoff frequency f_c.

- **Low-pass Filter**

  A low-pass filter passes low frequency signals from 0 Hz to its cut-off frequency f_c. Signals with a higher frequency range are blocked. This filter is considered the opposite of a high-pass filter.

- **Band-pass Filter**

  A band-pass filter is considered a combination of a low-pass and a high-pass filter. This filter allows signals within certain frequency ranges to pass, while signals with frequencies below and above this range are blocked.

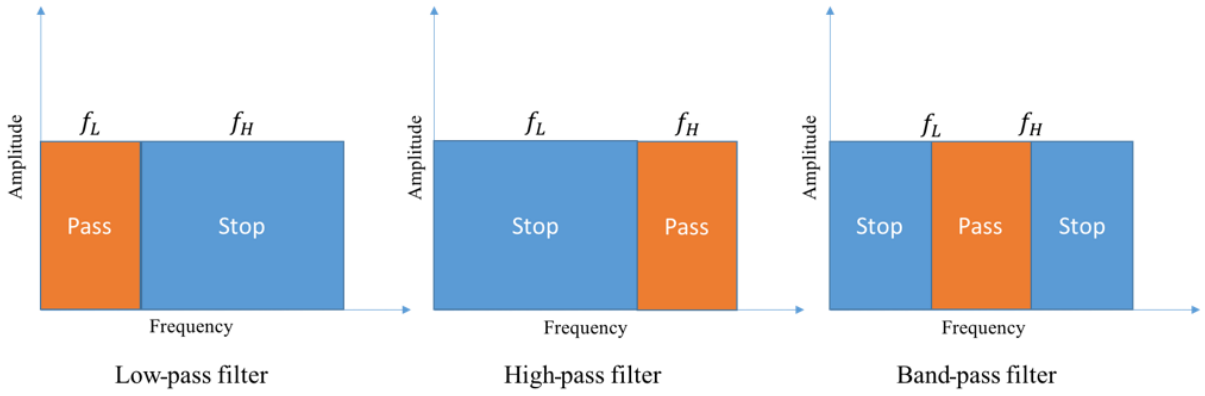

Figure 2-8 Filter design illustration: low-pass filter, high-pass filter, and band-pass filter

In addition to filters, Fast Fourier Transform (FFT) plays an important role in signal processing, and it was included in the Top 10 Algorithms of the 20th century by the IEEE journal Computing in Science & Engineering [26]. FFT is a mathematical tool for transforming a function of time into a function of frequency. Sometimes it is described as transforming from the time domain to the frequency domain. The Fourier transform accomplishes this by breaking down the original time-based waveform into a series of sinusoidal terms, each with a unique magnitude, frequency, and phase. Figure 2-9 shows an example of how a function (2-5) is transformed from time domain to frequency domain using Fast Fourier Transform.

$$x = 0.7\sin(2\pi w_1 t) + \sin(2\pi w_2 t) + 1.3\sin(2\pi w_3 t) \quad (2\text{-}5)$$

where $w_1 = 50$ Hz, w_2=120 Hz, and w_3=300 Hz.

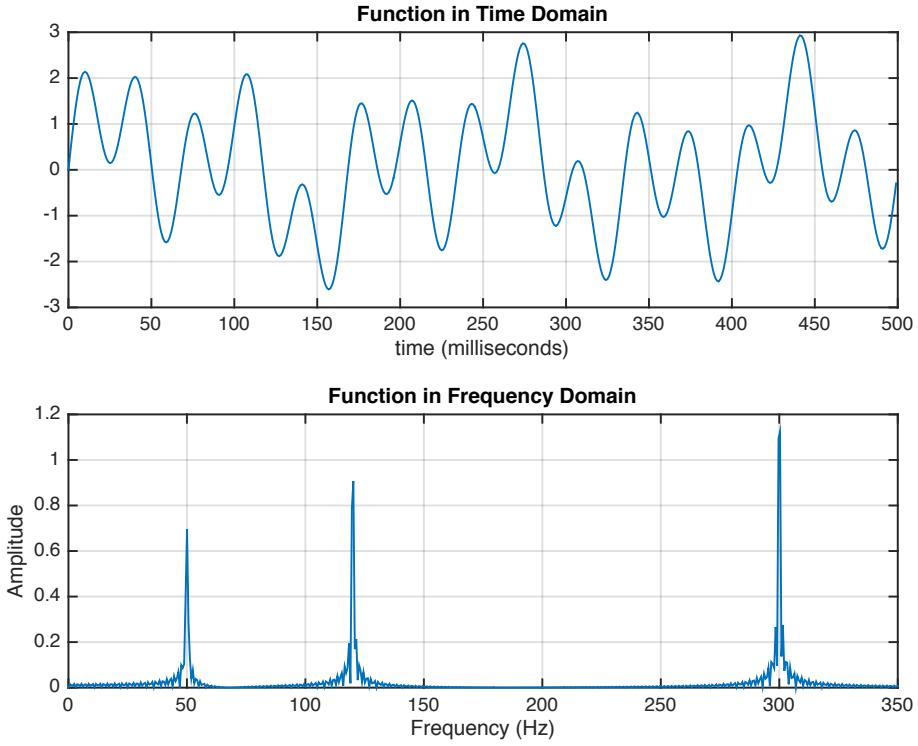

Figure 2-9 A function in time and frequency domain

Chapter 3
Experimental Setups

This chapter explains the installation procedures of the Laser Sensor system to test in two locations: first, on a lab Rail Track panel, and then on a cart surveying a 250-ft rail section in a yard. Laboratory track panel tests are conducted to evaluate the applicability of the system for detecting TOR lubricants in a controlled environment. The data collected during the lab tests are processed using signal-processing algorithms to obtain the maximum signal-to-noise ratio, and to quantify the effect of each parameter individually. Yard rail tests are conducted to verify the laboratory test results, and to assess the system's ability to detect various types and amounts of lubricants in outdoor conditions. The results are presented in the next chapters.

3.1 Lab Track System Setup

A 40-ft track panel at the Railway Technologies Laboratory (RTL) of Virginia Tech (VT) is used to conduct an initial round of testing with the laser-based measurement system. Twenty feet of the track panel are used for the testing system. The test section is divided into shorter sections to test three commercially-available TOR lubricants. A red reflective tape is used as an optical separator for the tests. The reflective tapes provide a maximum amount of reflection that appears as a large voltage spike in the system's output. The spikes serve as separators for various sections of the test track.

Each section of the test rail is scanned at least twice: once under unlubricated conditions and another time under lubricated conditions. The unlubricated rail sections are used as reference to compare with the lubricated sections. Three lubricants that are used by the U.S. railroads in revenue service are obtained and used for testing. In order to maintain the anonymity of the lubricant suppliers, they are referred to as Lubricants A through C, with specifications for each

provided in Appendix A. Each sub-section is lubricated by one of the three lubricants, which lubricants are applied manually, using a paint roller. To achieve thinner layers, a dry roller is used to absorb some of the applied lubricant. Applying the dry roller in successive steps and making measurements in between each step allow us to collect data for various states of lubricity.

The laser sensor is composed of two important pieces: a laser head and an amplifier. The laser head sends and receives beams to the object with an adjustable focal length. That is, the distance from the laser head to the object can vary from 200 mm to 1200 mm. It is installed so that the laser beam is perpendicular to the surface and is received as a specular reflection. Differences between specular and diffuse reflection are explained later. In this application, the laser head is mounted 3.5 ft. above the TOR. The laser head is installed at the leading part of the cart so that the scanning is done before the lubricant is touched by the cart wheels, which minimizes the effect of the cart on the measuring process.

The amplifier has an analog output that ranges from 1V to 5V. Therefore, a high-intensity signal (as received from red reflective tape) will always record 5V, and a low-intensity signal (as received from a black matte object) will always record 1V. This is why it is important to install the laser head at the correct height: the height of 3.5 ft. assures that the output signal is always between 1V and 5V. The laser used for the tests is a Class 1 laser product according to FDA (CDRH), which is skin and eye safe. It has 660 nm wavelength, which is visible with an output of 310 μW.

This system is connected to a DAQ that is directly connected to a laptop that shows a live plot of how the signal is changing with time. All these components are mounted on a cart that can be moved remotely and is powered with rechargeable batteries.

3.2 Field Track System Setup

A 250-ft. yard rail is used for testing. This section of rail, shown in Figure 3-1, is curved and has some short sections. The laser sensor has several components. The laser head, which sends and receives the laser beam, is located 3 ft. above the rail, as shown in Figure 3-2. This laser sends a 660-nm beam with an adjustable focus so that it can be mounted anywhere between half a foot to 4 ft. above the rail. The closer the head is to the subject, the higher reflective intensity is received. The amplifier outputs a voltage that is always between 1V and 5V; as discussed previously, it is important to choose a proper location for the laser head to assure that the output is between these two values.

Figure 3-1 Yard curved section of track

Figure 3-2 Laser head mounted 3 ft. high with respect to rail

Figure 3-3 shows the entire cart that is used to scan, measure, and detect rail lubrication. The laser processing system, composed of a laser amplifier, DAQ, and a laptop, is located on the cart and is powered by rechargeable batteries. The laptop screen is used to monitor changes in specular reflection signals, which helps in adjusting the location of the laser pointer to obtain maximum reflection signals. The cart is moved using remote control in order to achieve a constant speed and consistent data rate.

Figure 3-3 Scanning cart with laser processing system on-board

To separate rail sections according to the applied lubricant, a red reflective tape is used to mark every 50 ft. of rail, as shown in Figure 3-4. This tape has the ability to reflect most of the laser

beam so that the output is always 5V. The red tape serves as a marker in the collected data in order to separate sections with different lubricants.

Figure 3-4 Red reflective tape acts as rail sections markers

Applying lubricant is not a controlled task. A thick layer of lubricant is applied using rollers, as shown in Figure 3-5. Lubricant is removed using a dry roller, and the rail is scanned after every step. The last measurement is made with a thin residue of the lubricant remaining, with the rail nearly resembling an unlubricated condition, as shown in Figure 3-6.

Figure 3-5 Applying TOR lubricants using small roller

Figure 3-6 A thin layer of Lubricant C on top of rail

The laser system is installed and lubricant detection tests are conducted for unlubricated and lubricated rails. The lubricants are applied manually and removed gradually to achieve various layers of thickness for each test. The test results are presented in the following chapters.

Chapter 4
Lab Track System Results

This chapter discusses the results of lubrication monitoring for different types of lubricants using laser technology on a lab track panel. A 40-ft rail panel at Railway Technologies Laboratory (RTL) of Virginia Polytechnic Institute and State University (VT) is used for lubrication detection tests. Three different commercially-available lubricants are used, and the results are compared.

4.1 Lubrication Detection

For lubrication detection and measurements on rails, specular reflection will be considered, as discussed in Chapter 7. A reference from an unlubricated rail is needed to act as a calibration for the sensor. Figure 4-1 provides the unlubricated rail specular reflection of one section of the track.

A low-frequency signal exists in Figure 4-1. Thus, Fast Fourier Transform (FFT) is considered to detect any low-frequency signals, as shown in Figure 4-2 and Figure 4-3. A spike at 0.498 Hz is detected, which may have been caused by rail surface irregularities. Since the frequency spike is immaterial to our measurements and its cause is not exactly known, it is eliminated from the data using a high-pass filter. Additionally, a moving average is used to better capture the data trend, as in Figure 4-4, for all tests.

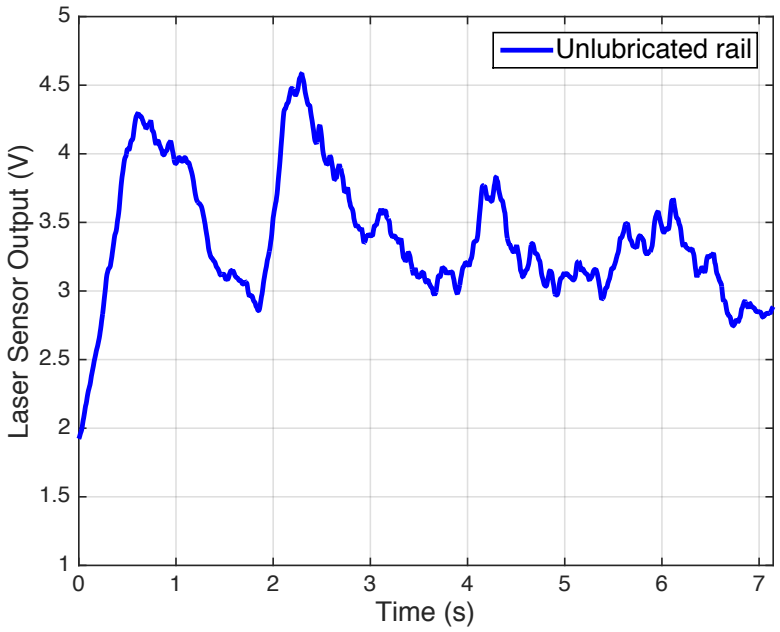

Figure 4-1 Lab track unlubricated rail specular reflection voltage

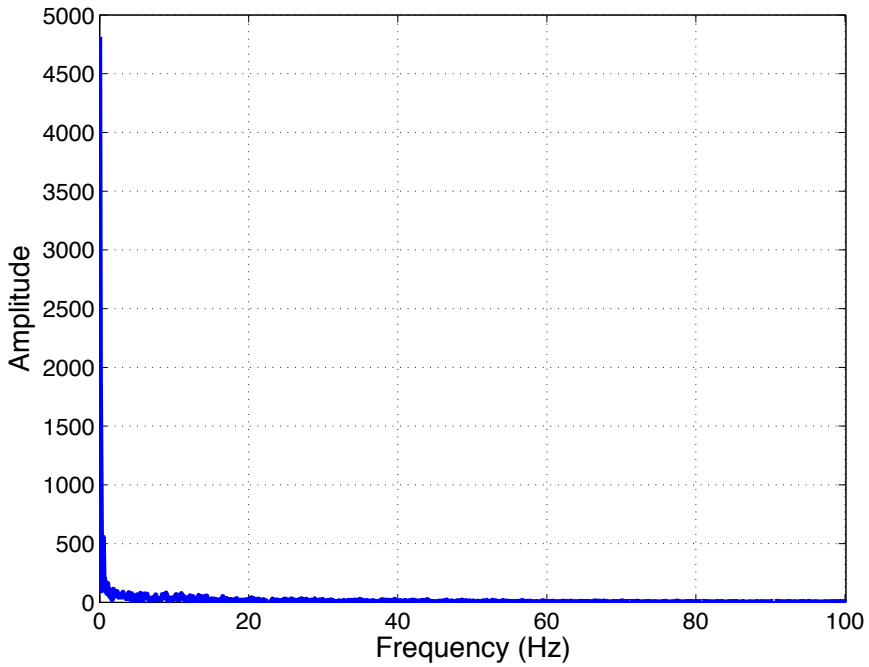

Figure 4-2 Lab track unlubricated rail specular reflection FFT

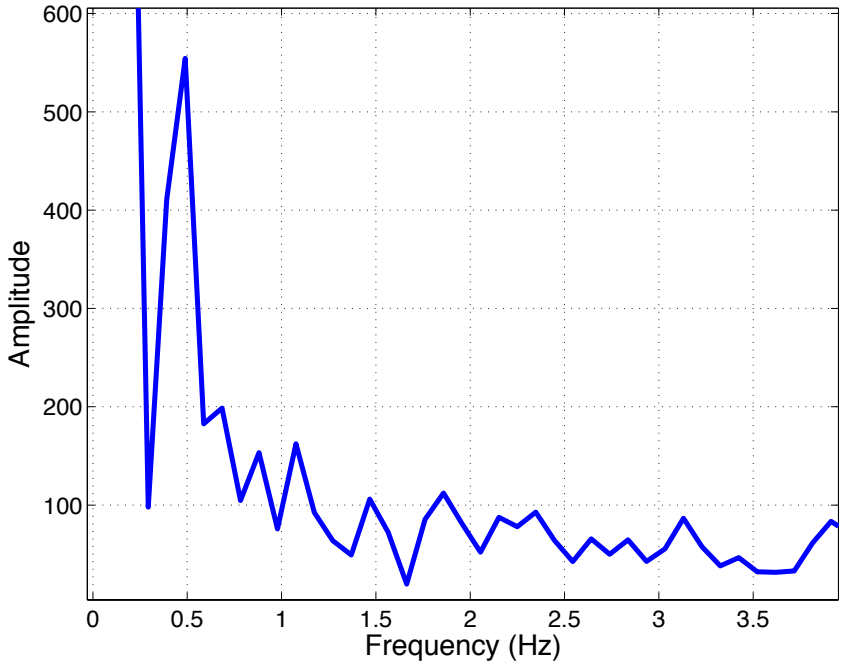

Figure 4-3 Lab track unlubricated rail specular reflection FFT magnified

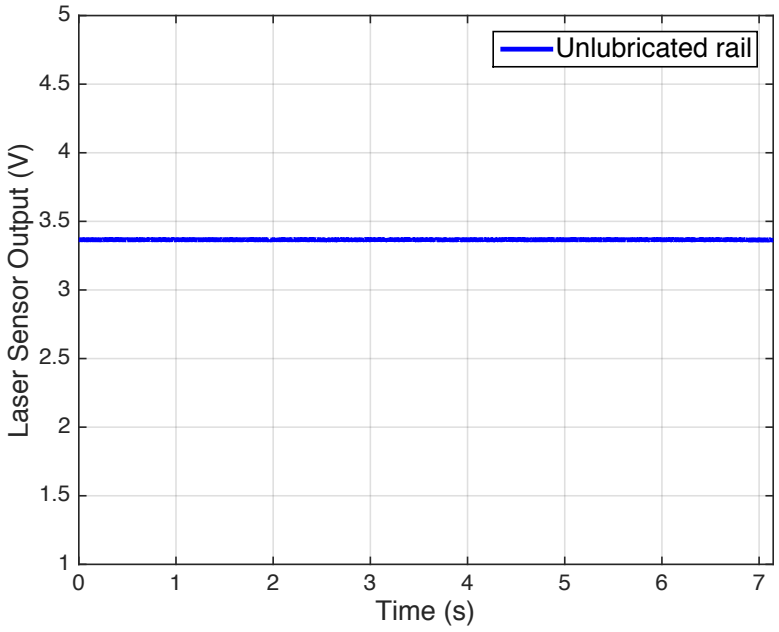

Figure 4-4 Lab track unlubricated rail specular reflection mean value with High-Pass filter

4.1.1 Lubricant A

Lubricant A is a water-based, liquid friction modifier applied using TOR application systems. When applied, Lubricant A is transferred to rail vehicles from the top of the rail and establishes dry thin film friction control at the wheel tread/top of rail interface. In its liquid form (prior to application), Lubricant A is similar in appearance and has some characteristics similar to water-based latex paint. When applied to the top of the rail, the liquid material is picked up by the train wheels and carried down the track. The water component dries rapidly, forming a dry thin film.

After applying Lubricant A to the lab track rail, a test was carried out to compare reflection of both unlubricated and lubricated surfaces. It is clear, as in Figure 4-5, that specular reflection of the lubricated surface has lower values compared to the unlubricated rail. Such a reduction in reflection is noticeable and detectable.

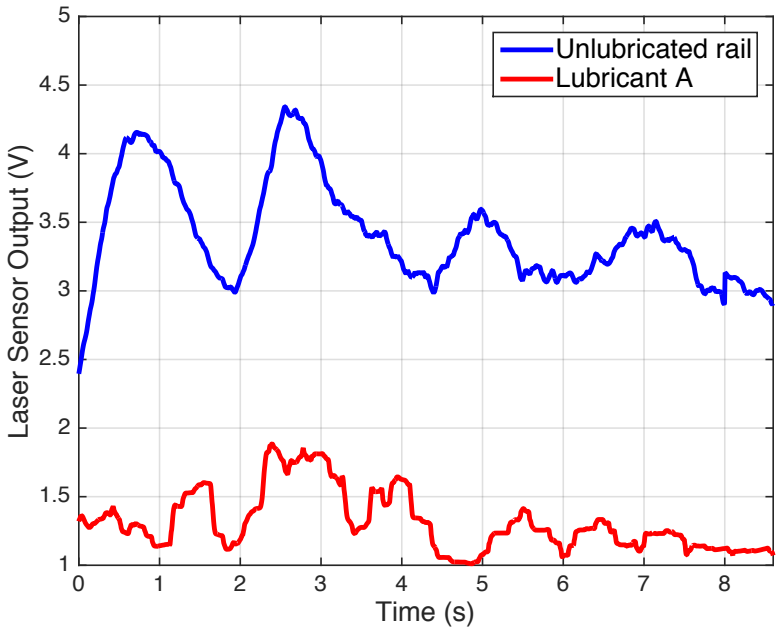

Figure 4-5 Lubricant A specular reflection compared to lab track unlubricated rail

To make results clearer and more obvious, a high-pass filter is applied. Figure 4-6 shows the large difference between a lubricated and unlubricated rail. The difference (or ratio) between the lubricated and unlubricated rail measurements is directly proportional to the amount of lubricant on the rail, although not necessarily in a linear fashion. The difference increases nonlinearly with increasing lubrication, for all lubricants, as will be discussed in later sections.

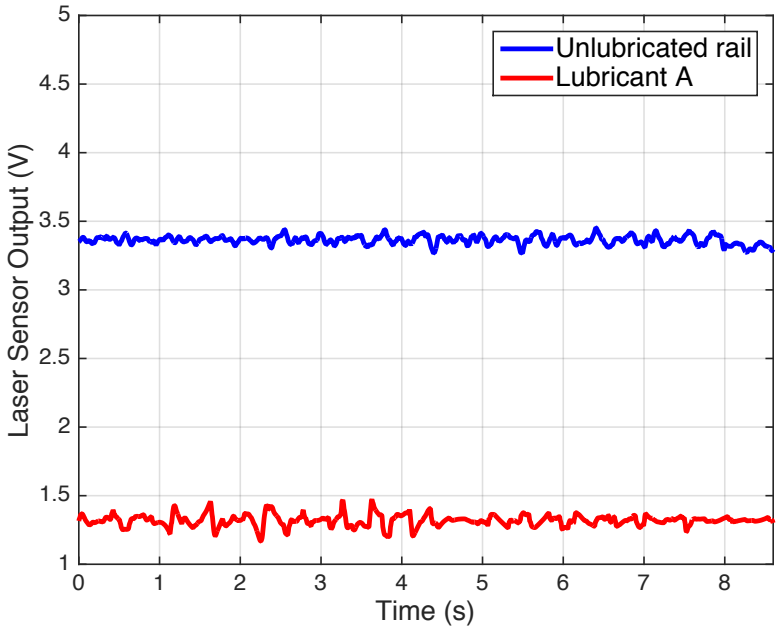

Figure 4-6 Lubricant A specular reflection mean value with High-Pass filter compared to lab track unlubricated rail

4.1.2 Lubricant B

Lubricant B is a top-of-rail friction modifier. During normal rolling, it acts as a lubricant. Nevertheless, when wheel creep occurs, the sliding friction immediately converts to "positive friction," controlling the creep condition and reducing lateral forces. Lubricant B contains no solvents or latex. It dries quickly between the wheel and the rail due to frictional heat.

Similar to Lubricant A, Lubricant B reduces laser specular reflection, as shown in Figure 4-7. Due to its black color, it absorbs most of the light, which makes it easily detectable by the laser beam.

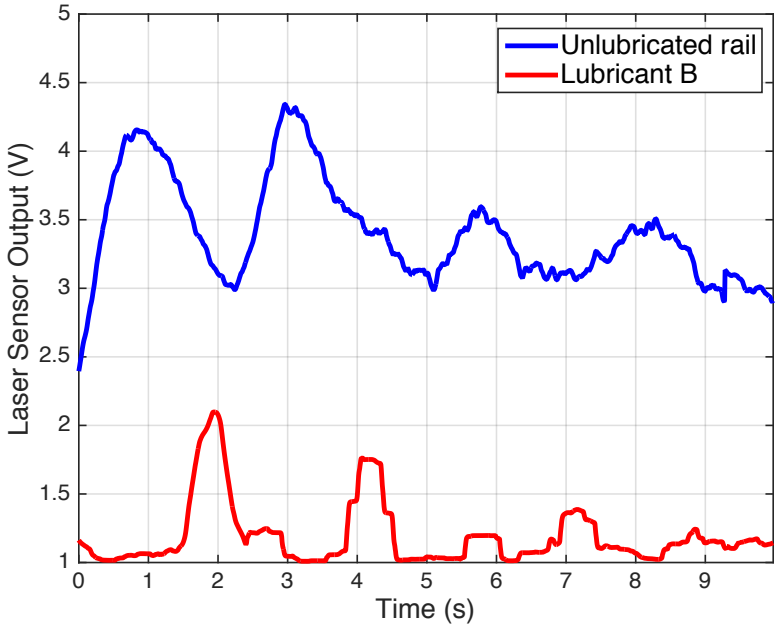

Figure 4-7 Lubricant B specular reflection compared to lab track unlubricated rail

To remove surface non-homogeneity effects, a high-pass filter is applied and combined with the mean value, as shown in Figure 4-8.

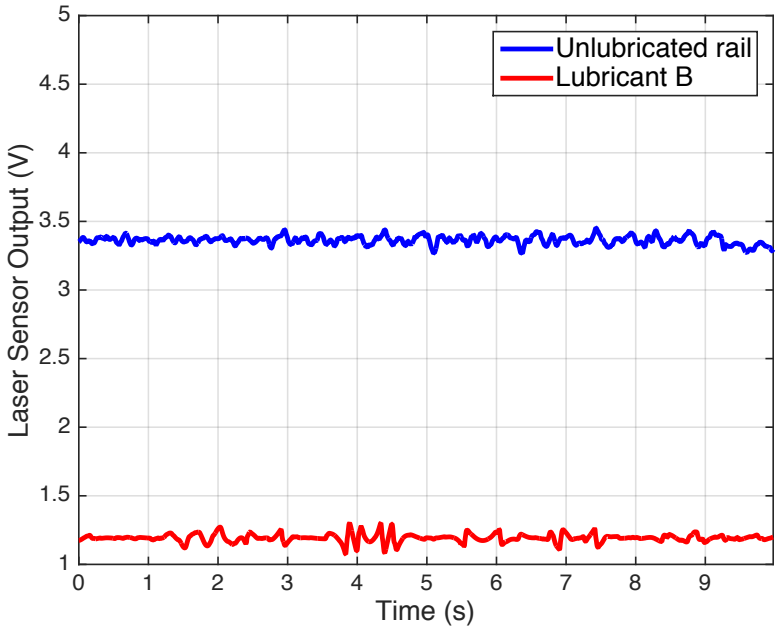

Figure 4-8 Lubricant B specular reflection mean value with High-Pass filter compared to lab track unlubricated rail

4.1.3 Lubricant C

Lubricant C is specifically developed for TOR and rail gauge corner applications. In addition to functioning as a friction modifier, Lubricant C concurrently serves as a freeze barrier to snow and ice.

Since Lubricant C is an oil-based transparent lubricant, results are different compared to the previous lubricants. Because of its transparent state, it does not absorb enough light. Thus, reflection values are higher compared to other lubricants, but still less than an unlubricated rail. Lubricant layer thickness does affect the results, as shown later in Chapter 7. It is also obvious how both signals have almost the same pattern, as shown in Figure 4-9, which does not exist in other lubricants. Slight differences in the correlation are because each test is done separately at slightly different speeds. Data post-processing is used to correlate results for the same rail position.

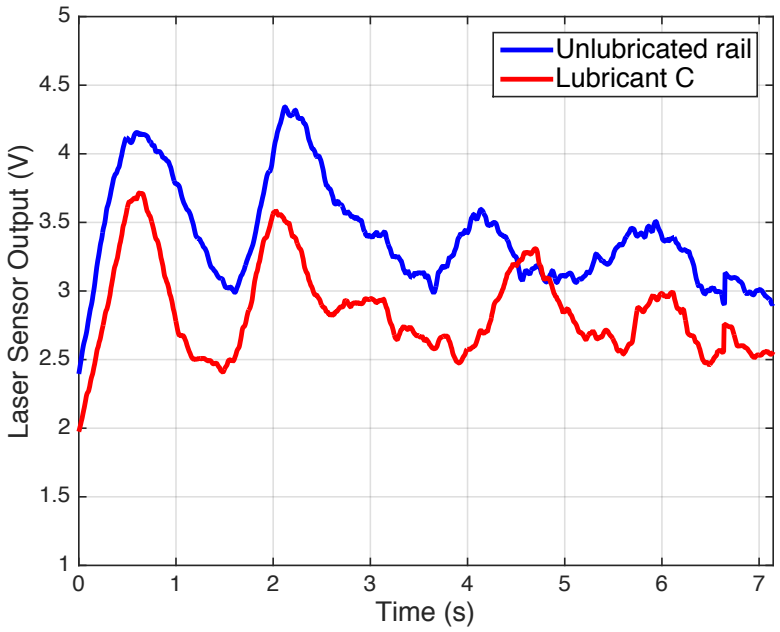

Figure 4-9 Lubricant C specular reflection compared to lab track unlubricated rail

To see the difference clearly, Figure 4-10 shows results after a high-pass filtering. Quantification of rail lubricity will be discussed in Chapter 7.

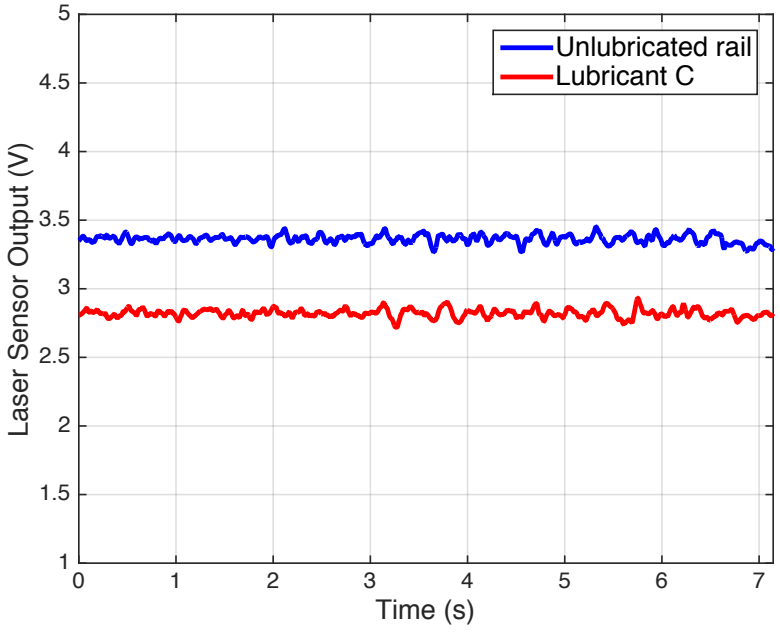

Figure 4-10 Lubricant C specular reflection mean value with High-Pass filter compared to lab track unlubricated rail

Chapter 5
Field Track Results

This chapter discusses the results of using the laser measurement system to evaluate the effectiveness of the system in detecting various amounts of TOR lubricant on a 250-ft curved section of track, with different types of commercially-available rail lubricants manually applied at varying amounts to the rail.

5.1 Lubrication Detection

Tests are done to detect lubricants on yard track similar to what is done with the Lab Track Panel. Lubricants A, B, and C are tested in various thickness layers. The effect of the lubricant layer thickness will be discussed in Chapter 7.

An unlubricated rail is tested first for reference and to calibrate sensors. Five sections, 50-ft. each, are scanned, as shown in Figure 5-1. The 5V spikes are the signals from the red reflective tapes that are used as separators for each section. These spikes will be used to detect and separate sections. Lubricants A, B, and C will be applied on sections 2, 3, and 4, respectively.

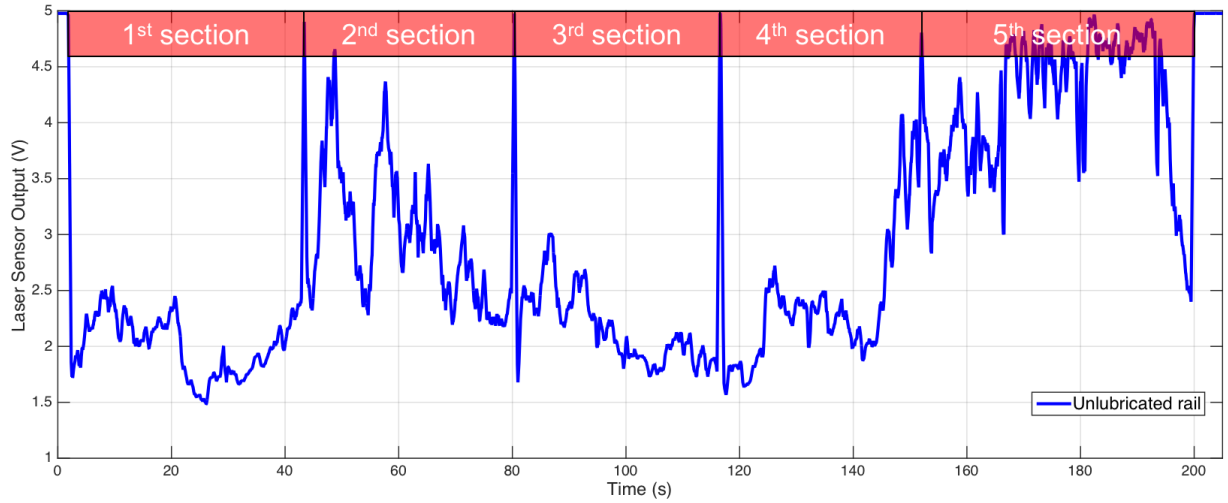

Figure 5-1 Specular reflection of yard rail in unlubricated condition

FFT is plotted to check the existence of any low-frequency signal and to justify the use of a high-pass filter. Figure 5-2 shows no spikes in any particular frequency, so there is no need to use a high-pass filter. A 50-point moving average will be used to smooth out the output voltage and better highlight the data trend.

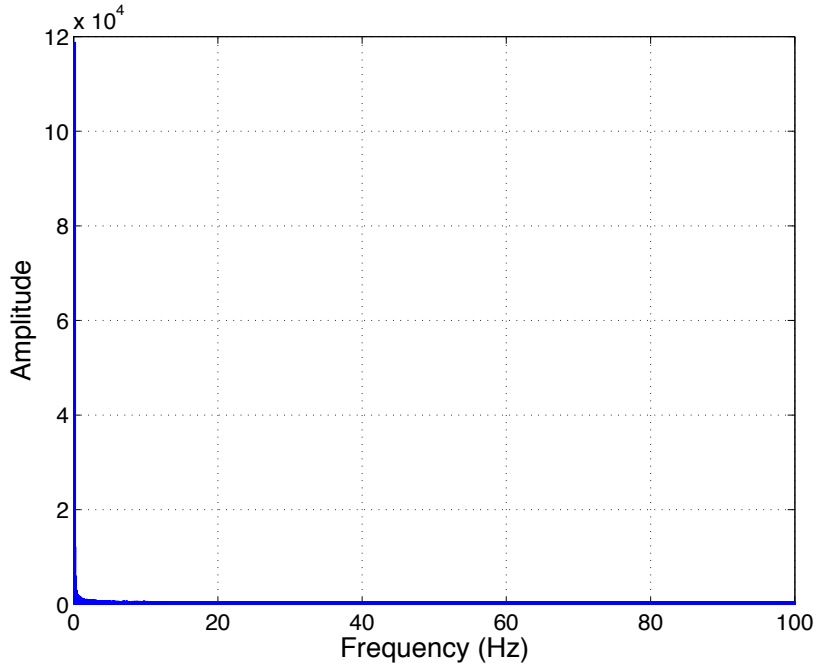

Figure 5-2 Yard unlubricated rail specular reflection FFT

5.1.1 Lubricant A

As mentioned earlier, section 2 of the rail is chosen for Lubricant A. The lubricant is applied and scanned using the laser sensor to measure specular reflection. Results are compared to the same section of the rail before the application (unlubricated). Figure 5-3 demonstrates the difference in the two signals. Due to its dark grey color, Lubricant A reflection signal has a different signature as compared with an unlubricated rail. It is worth mentioning that Lubricant A dries fast, within minutes of application. This test was done after it dried, so the amount of lubrication applied is greater compared to the actual recommended amount. This difference in thickness layer will be discussed later.

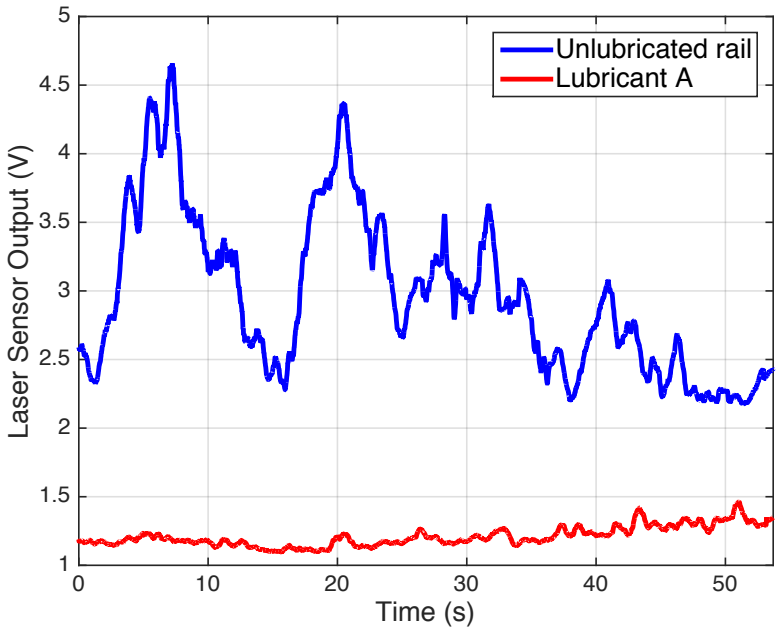

Figure 5-3 Lubricant A specular reflection compared to yard unlubricated rail

5.1.2 Lubricant B

Section 3 of the rail is used to test Lubricant B. Similar to Lubricant A, it is easy to distinguish between the specular reflection signals of the unlubricated rail and Lubricant B. Lubricant B has a lower specular reflection due to its ability to absorb light, since it is a thick black

lubricant. Figure 5-4 illustrates these differences and how Lubricant B compares to unlubricated rail. Reflection is significantly lower than the unlubricated rail reflection signal.

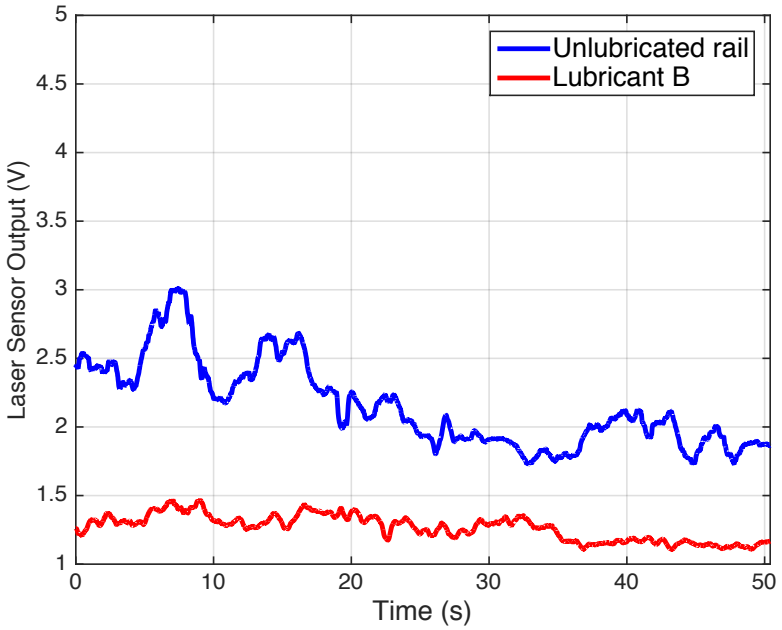

Figure 5-4 Lubricant B specular reflection compared to yard unlubricated rail

Tests are done with several thickness layers of Lubricant B. Since Lubricant B takes a long time to dry, it is feasible to add and remove several layers and then test each case individually. As shown in Figure 5-5, a lower amount of lubrication causes a higher amount of reflection off the top of the rail, resulting in a higher voltage output. A higher amount of lubrication causes more dispersion of the laser beam, and results in a lower voltage output. Therefore, Figure 5-5 indicates that there is a direct correlation between the specular reflection and the amount of lubrication on the rail.

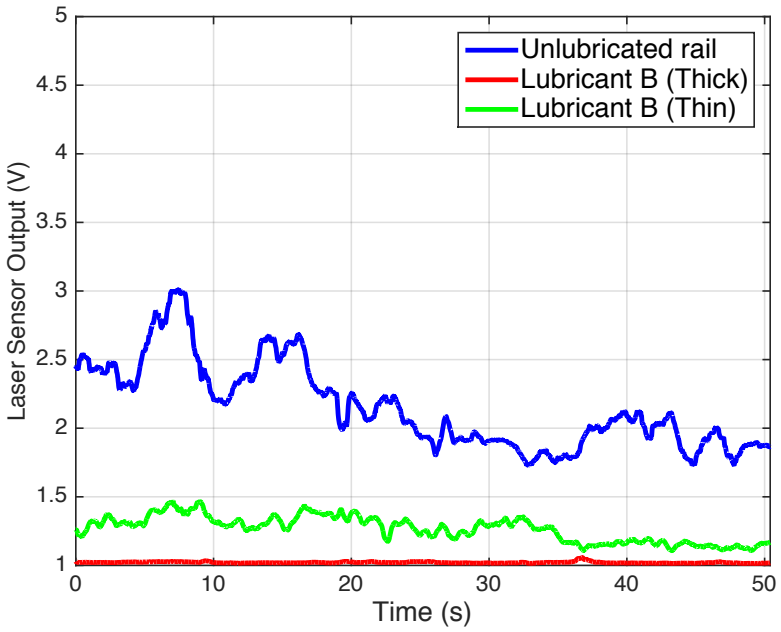

Figure 5-5 Different layer thicknesses of Lubricant B compared to unlubricated rail specular reflection

5.1.3 Lubricant C

Unlike the previous lubricants, Lubricant C, as mentioned earlier, is an oil-base transparent lubricant. Thus, light can penetrate and reach the rail surface, which allows it to scan rail surface irregularities, as shown in Figure 5-6. The correlation between unlubricated rail and Lubricant C specular reflection signals shows that the laser is able to detect the variation and small differences of rail surface in both cases. Lubricant C has a relatively high reflection compared to other lubricants because its ability to absorb light is minimal, which will make the process of identifying and quantifying lubrication more difficult. Thus, it is important to set a systematic way (as will be discussed later) to quantify accurately the amount of lubricant on the rail.

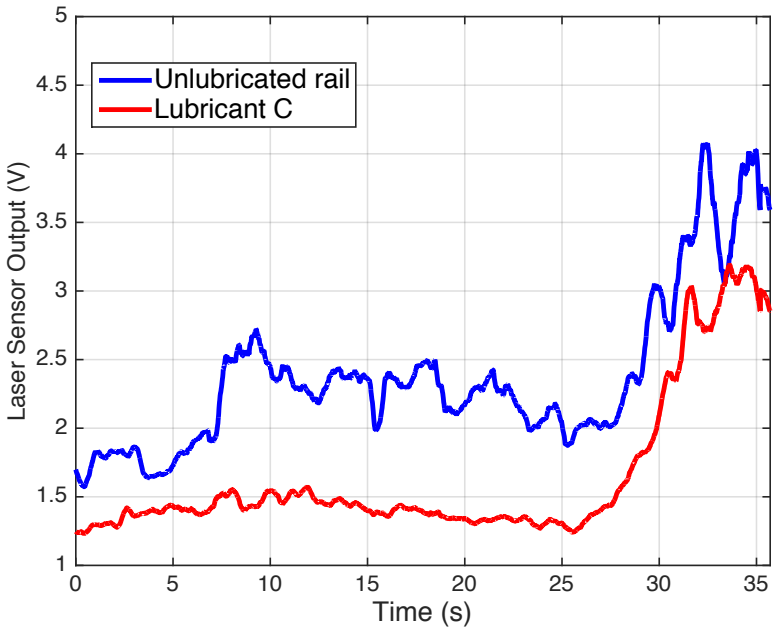

Figure 5-6 Lubricant C specular reflection compared to yard unlubricated rail

Chapter 6
Revenue Service Track Testing

This test is intended to evaluate the effectiveness of the laser system on revenue service track, under conditions commonly existing in the field and with an actual wayside lubricant applicator in use instead of applying lubricants by a roller. The tests are done at a location near Roanoke, Virginia. The test details and preparation plans will be discussed in the following sections.

6.1 Plan and Preparation

A section of revenue service track, approximately 2500 ft in length, with a tangent and two curved rails, was selected for testing. Most of the rail was subjected to direct sunlight, with the exception of a bridge section that was completely shaded. Two tests were done on the same section of the rail: southbound and northbound. Southbound tests use the high rail to measure and detect lubrication and light reflection. Northbound tests, however, use the low rail. Figure 6-1 shows a map of the test site, which also includes train direction, lubricator location, pictures of some test rail, and weather and light conditions in each section.

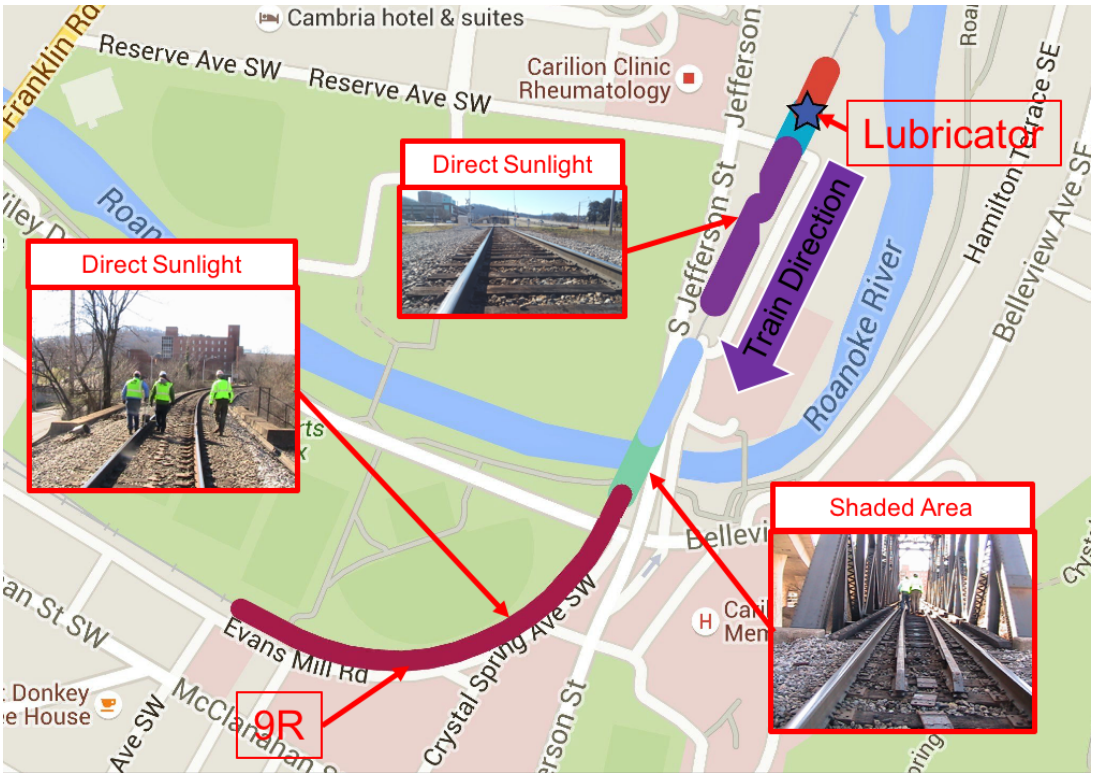

Figure 6-1 Test site map, location, train direction, and pictures of test track sections

A wayside lubricator, as shown in Figure 6-2 and Figure 6-3, is used for lubricating the top of the rail. A train passed by the lubricator and carried the lubricant to spread it on the rail heading south. The test track was divided into different sections according to luminance level and lubrication condition, as shown in Table 6-1. The southbound tests start with section 1 and end with section 4. The northbound tests start and end in reverse order, starting with section 4 and ending with section 1. In order to have symmetrical results, the northbound test results are flipped, spatially, to match the southbound results.

Figure 6-2 Wayside lubricator station near test rail

Figure 6-3 Close-up picture of the lubricator pumping lubricant on top of rail

Table 6-1 Track sections in southbound and northbound tests

Section #	Lubrication condition	Luminance level	Track shape	Length (ft.)
1	Unlubricated	Direct sunlight	Tangent	140
2	Lubricated	Direct sunlight	Tangent	780
3	Lubricated	Shaded	Tangent	210
4	Lubricated	Direct sunlight	Curved	1350

6.2 Setup and New Cart

The cart is modified to have better stability and reliability, especially in curved sections. In addition, an encoder is added to enable measurement of the spatial position of the tests along the track. Figure 6-4 shows the new modified cart, which includes a push handle for pushing the cart at walking speeds along the track. This is in contrast to the earlier design of the cart that included a motor-driven wheel with a remote control unit, used for remotely operating the cart.

Figure 6-4 Modified cart equipped with laser sensor, encoder, and data acquisition system

Different sets of rollers and wheels are added to the cart for different purposes. The front and back wheels are installed for motion and cart stability. They are shifted by a small margin from the centerline of the rail to minimize their effect on rail lubrication. To minimize cart yaw motion, an additional wheel is placed on the other side of the rail, as shown in Figure 6-4. A system of rollers and springs are added to grip the rail from the sides. This allowed the laser pointer to be spotted at the same location all the time, and also minimized unwanted side-to-side motion on curves that existed in the previous cart.

The cart was tested at different walking paces to check its reliability at various operating speeds. Figure 6-5 shows a sample of cart velocity testing on an unlubricated tangent track. The cart was pushed at low speeds (about 1 – 1.5 mph) to test the first section and to make sure that the cart was reliable. This section was tested at an average of around 1.2 ft/s.

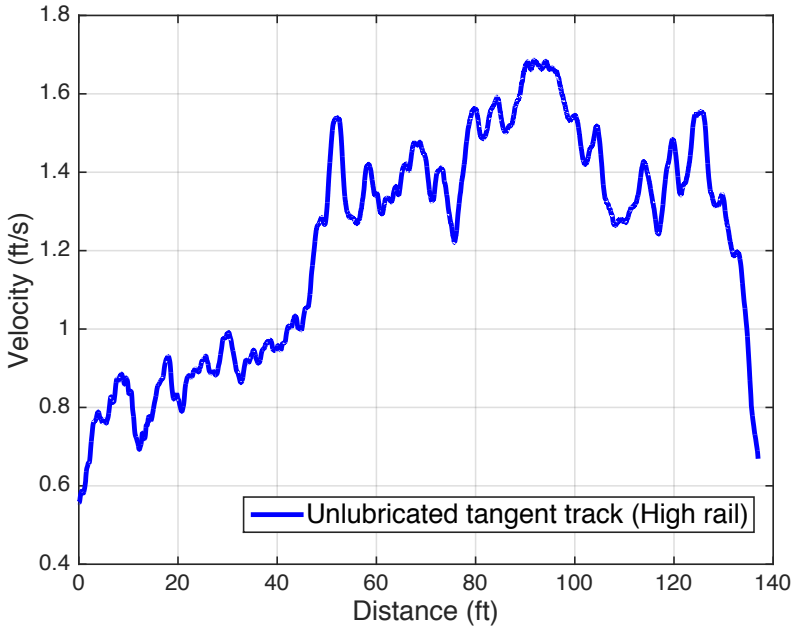

Figure 6-5 Velocity of a manually-pushed cart on an unlubricated tangent track

After testing many sections of the track, the cart was pushed at higher speeds, as shown in Figure 6-6. The average speed in this curved lubricated section is around 4 ft/s. It is worth mentioning that the sampling rate in this test is 900 Hz. The sampling rate can be set as high as 7200 Hz by reducing the number of channels of acquired data. The current setup uses eight channels, which can be reduced to only one channel that outputs the reflection values. The sampling rate of 900 Hz was determined to be sufficiently high for the speeds at which the cart was operated.

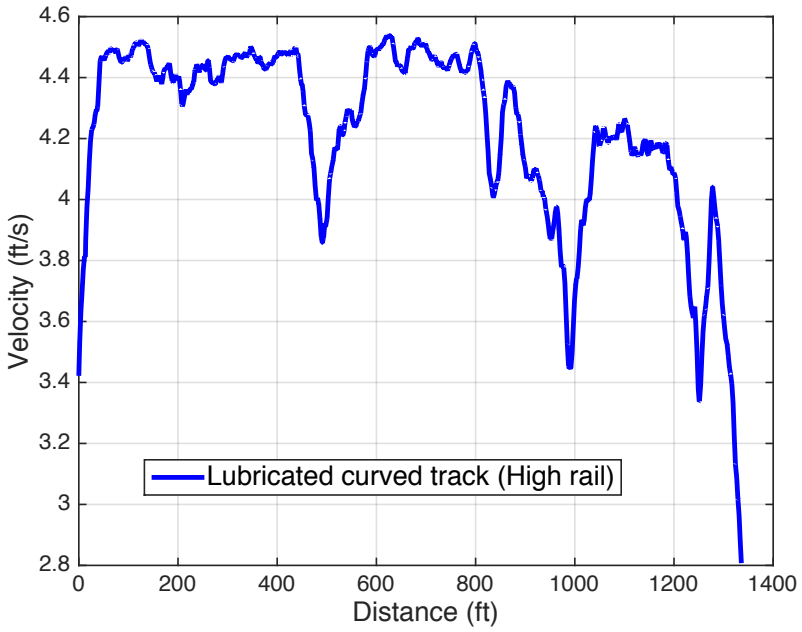

Figure 6-6 Velocity of a manually-pushed cart on a lubricated curved track

6.3 Results and Data Analysis

Unlike results presented in previous chapters, same-section comparison cannot be done because of the test conditions and plan. Instead, a comparison is made between different sections of the same track. Figure 6-7 shows rail reflection, represented as laser sensor output, of a full track test with details about lubrication and weather conditions. Each section will be explained and discussed individually and then compared to each other. It is important to mention that this figure represents the test done using high rail while heading south (i.e. southbound test).

The first section tested is the unlubricated tangent track, as shown in Figure 6-8. This section was under direct sunlight and located just before the wayside lubricator. This section was part of the southbound test, which means that the high rail was scanned here. The mean value of the laser sensor output (reflection) is around 3.1V. This information will be used to compare with lubricated sections later in this chapter.

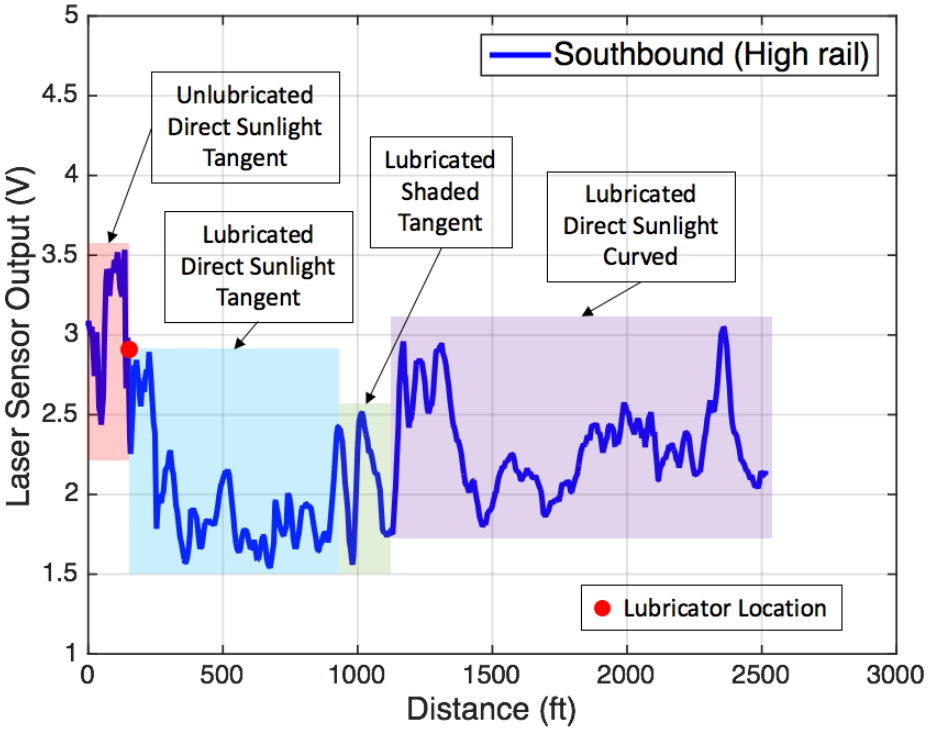

Figure 6-7 Laser sensor output of the southbound track test with different lubrication and luminance conditions

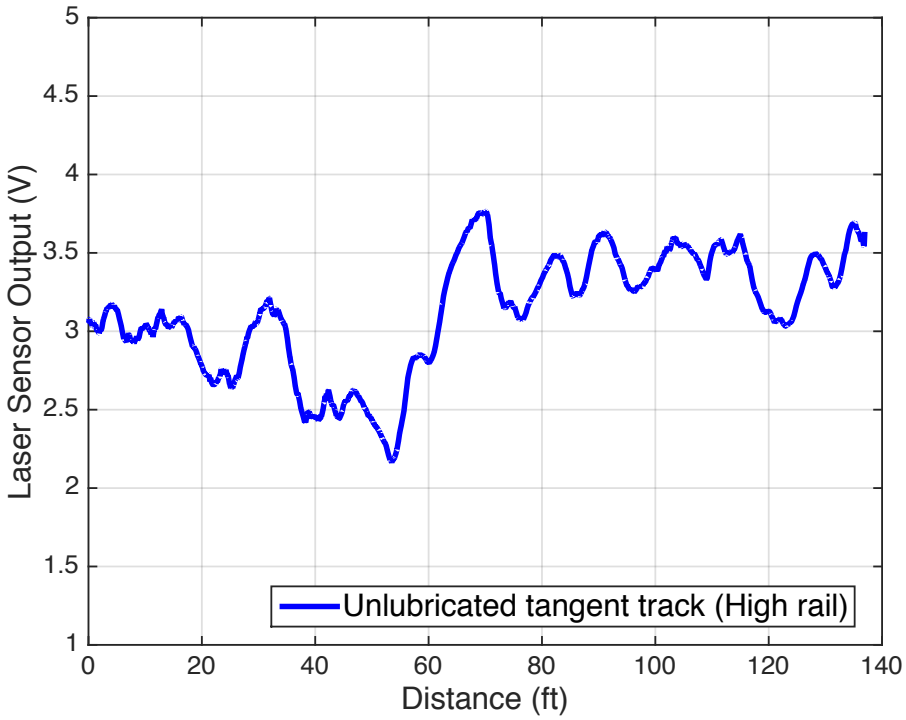

Figure 6-8 Laser sensor output of an unlubricated tangent track in the southbound test (high rail)

The second section of the southbound test was a lubricated tangent track, located after the wayside lubricator. It included two different luminance conditions: direct sunlight and shaded sections. Figure 6-9 shows reflection values of the lubricated high rail of a tangent track. The mean value of the rail reflection of this section is around 2V.

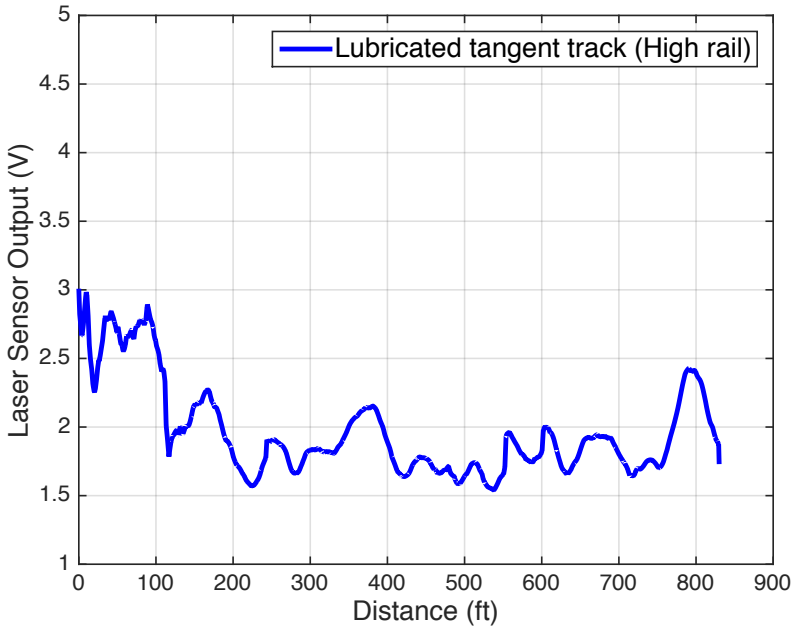

Figure 6-9 Laser sensor output of a lubricated tangent track in the southbound test (high rail)

It is obvious that the reflection values, shown in Figure 6-9, drop after the first 100 ft. The reason behind this lies how the wayside lubrication system works. The wayside lubricator pumps an amount of lubricant at only one spot on top of the rail. The train passes on that spot and its wheels carry the lubricant forward on the track. These wheels re-apply this lubricant on top of the rail with each rotation, creating discrete patches on the rail, as shown in Figure 6-10. Once all wheels contact these lubricant patches, the patches become closer to each other until it becomes a continuous lubricated section. This is where the drop in reflection value appears.

The third and last section of the southbound test was the lubricated curved track. With an average reflection value of 2.3 V, Figure 6-11 shows that even for a curved track, the reflection value is lower compared to the unlubricated track. This means that the laser is capable of detecting differences in reflection values according to the rail lubrication condition. It is worth

mentioning that the average value of this curved section is higher than that of the lubricated tangent section. The reason behind this difference will be discussed later in this chapter.

Figure 6-10 Section of the rail after the lubricator showing discrete patches of lubricant

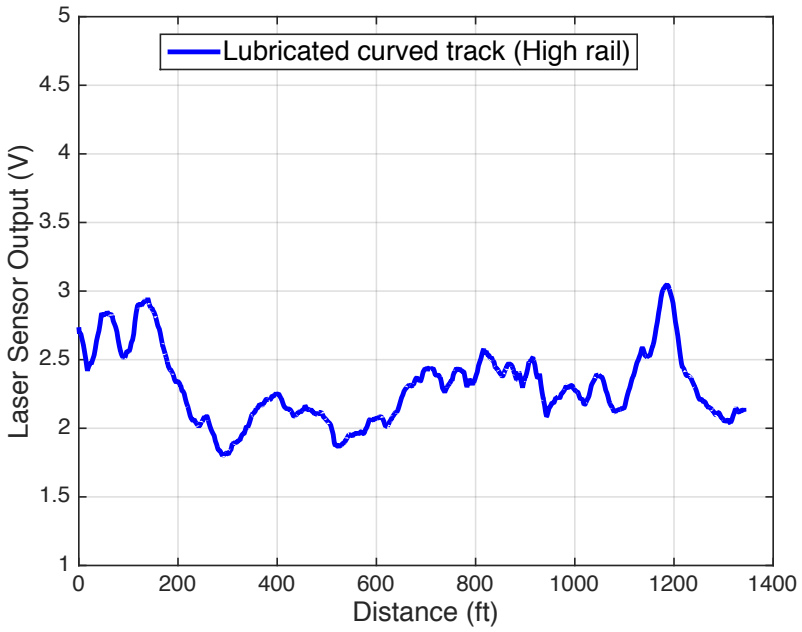

Figure 6-11 Laser sensor output of a lubricated curved track in the southbound test (high rail)

Table 6-2 shows the average values of the laser sensor output that represent reflection value of all southbound test sections. Unlubricated rail has higher reflection values when compared to lubricated rails, both tangent and curved. This difference, around 1V, is enough to detect lubricant on top of the rail.

Table 6-2 Average values of the laser sensor outputs in the southbound test for each section

Track section	Laser sensor output mean value (V)	Difference from unlubricated (V)
Unlubricated	3.101	0
Lubricated tangent	2.025	+1.076
Lubricated curved	2.299	+0.802

After the southbound test was completed, the northbound test started with an adjustment to the cart. The laser sensor was lowered approximately 6 inches and the cart was rotated. Lowering the laser position ensured that all the data points are above 1V, since it cannot output any value less than 1V. The lubricated tangent track has some values close to 1V, so lowering the laser sensor will raise the data points. The reason behind rotating the cart is to test the low rail instead of the high rail, and then compare the results.

As mentioned earlier, all data points are flipped to have similar results represented as compared to the southbound test. The unlubricated tangent rail has high reflection values with an average of 4.3 V, as shown in Figure 6-12, which is higher than the lubricated tangent section reflection values shown in Figure 6-13. The difference between their average values is around 1V, which is similar to the results found in the high rail southbound test.

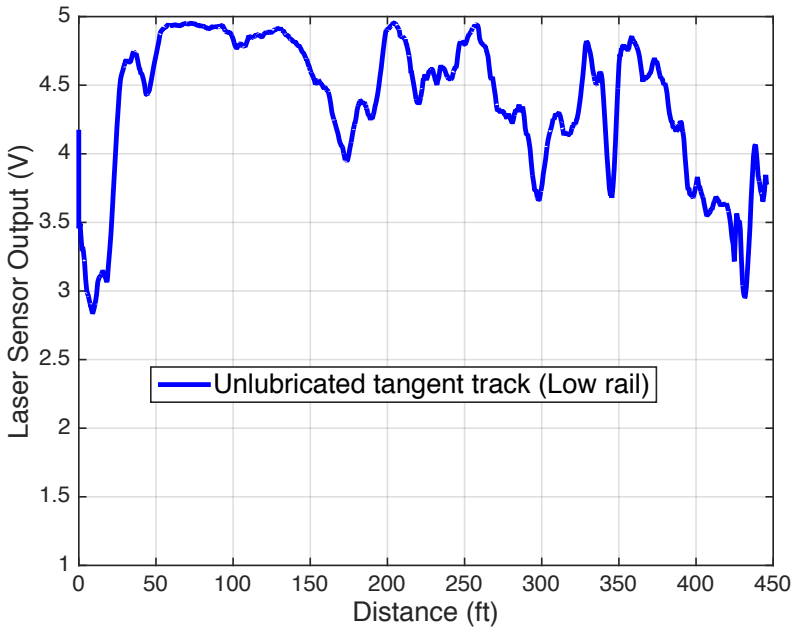

Figure 6-12 Laser sensor output of an unlubricated tangent track in the northbound test (low rail)

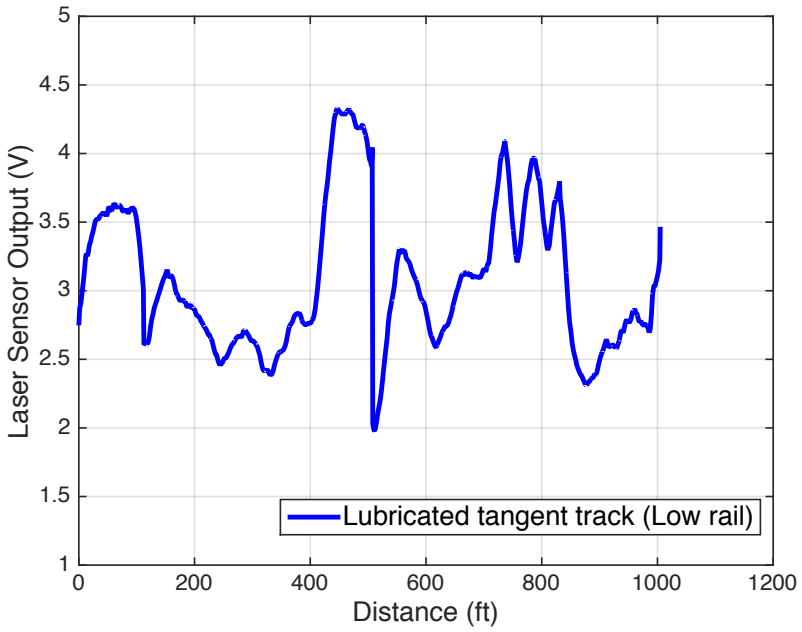

Figure 6-13 Laser sensor output of a lubricated tangent track in the northbound test (low rail)

Unlike the high rail, the low rail of the lubricated curved track had lower reflection values when compared to the lubricated tangent track: 2.2 V for curved, and 3.2 V for tangent track.

Figure 6-14 shows the laser sensor output of the lubricated curved track. When comparing all northbound test sections as shown in Table 6-3, it is obvious that the average reflection values of the unlubricated section are higher than both the lubricated tangent and curved sections by at least 1V. This shows how capable the laser sensor is in detecting top of the rail lubricants. The dryer the rail, the higher the reflection values. In addition, it shows that there is a difference in the amount of lubricant on top of the rail between the curved and tangent tracks. The low rail of a curved track is more lubricated than the tangent track according to the data collected by the laser sensor.

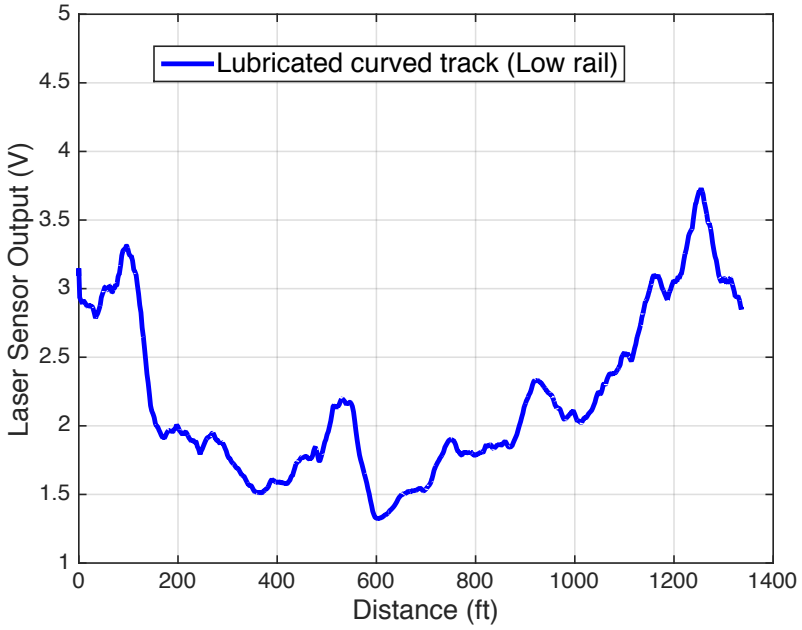

Figure 6-14 Laser sensor output of a lubricated curved track in the northbound test (low rail)

Table 6-3 Average values of the laser sensor outputs in the northbound test for each section

Track section	Laser sensor output mean value (V)	Difference from unlubricated (V)
Unlubricated	4.284	0
Lubricated tangent	3.193	+1.091
Lubricated curved	2.231	+2.053

To combine both the southbound and northbound tests, an adjustment has to be made since the laser sensor is not in the same location and height in both tests. Therefore, southbound data points are shifted so that the average reflection value of the southbound unlubricated tangent track is equal to that of the northbound unlubricated tangent track. This decision is made because both sections are at exactly the same lubrication and luminance conditions, which means that they should have the same reflection values. This shift value, which is equal to 1.2 V, is added to all southbound test sections.

Table 6-4 shows the shifted averages of the laser sensor output of both southbound and northbound test sections. As mentioned earlier, the reflection data of the unlubricated rail is higher than that of the lubricated rail. This is valid for both tangent and curved track, and for high and low rails. It is noted that for the high rail, the curved track has higher reflection values compared to the tangent track. On the other hand, for the low rail, the curved track has lower reflection values compared to the tangent track. To explain this, creepage of two rolling bodies must be presented:

$$v_x = \frac{\boldsymbol{c_w} - \boldsymbol{c_r}}{\frac{1}{2}(\boldsymbol{c_w} + \boldsymbol{c_r})} \tag{6-1}$$

where v_x is the creepage in the longitudinal direction, $\boldsymbol{c}$ is the circumferential velocity vector, and subscripts w and r denote the wheel and rail properties, respectively.

For the high rail, the circumferential velocity of the rail, $\boldsymbol{c_r}$, is greater than that of the wheel, $\boldsymbol{c_w}$, which leads to breaking creepage (i.e. negative creepage v_x). The presence of breaking creepage means that the wheel has more sliding time compared to the tangent track with no creepage. This causes the wheel to have fewer rotations on the rail. The less the wheel rotation, the less chance to spread the lubricant on the rail. This explains why the curved high rail is less wet, less lubricated, and more reflective compared to the tangent high rail.

On the other hand, the circumferential velocity of the wheel, $\boldsymbol{c_w}$, is greater than that of the rail for a low rail. This difference causes a traction creepage (i.e. positive creepage), which makes

the wheel spin in place more when compared to the tangent track with no creepage. The wheel in this case has more rotations on the rail, which increases the chances to spread the lubricant on top of the rail. This is the reason why the average value of the lubricated curved low rail signal is lower than that of the tangent low rail, as shown in Table 6-4.

Table 6-4 Shifted average values of the laser sensor outputs for southbound and northbound test sections

Track section	Northbound laser sensor output mean value (V)	Southbound laser sensor output mean value (V)	Shifted southbound laser sensor output mean value (V)
Unlubricated	4.284	3.101	4.284
Lubricated tangent	3.193	2.025	3.208
Lubricated curved	2.231	2.299	3.414

In order to develop a systematic way for quantifying rail lubricity, a new quantification method is presented. Lubricity Index $\mathcal{L}$ is a measure of the degree to which the rail lubricated compared to an unlubricated rail:

$$\mathcal{L} = R_D - R_x \tag{6-2}$$

where $\mathcal{L}$ is the Lubricity Index, R_D is the unlubricated rail reflection, and R_x is the reflection at point x. Table 6-4 is transformed using this equation into Figure 6-15. The unlubricated rail Lubricity Index is zero, and the other lubricated sections have higher indices accordingly. The greater the index, the more lubricated the rail. It is worth mentioning that a baseline (unlubricated rail) has to be tested and set as a reference for each test track in order to use this quantification method. Other methods will be explained and discussed later in Chapter 8.

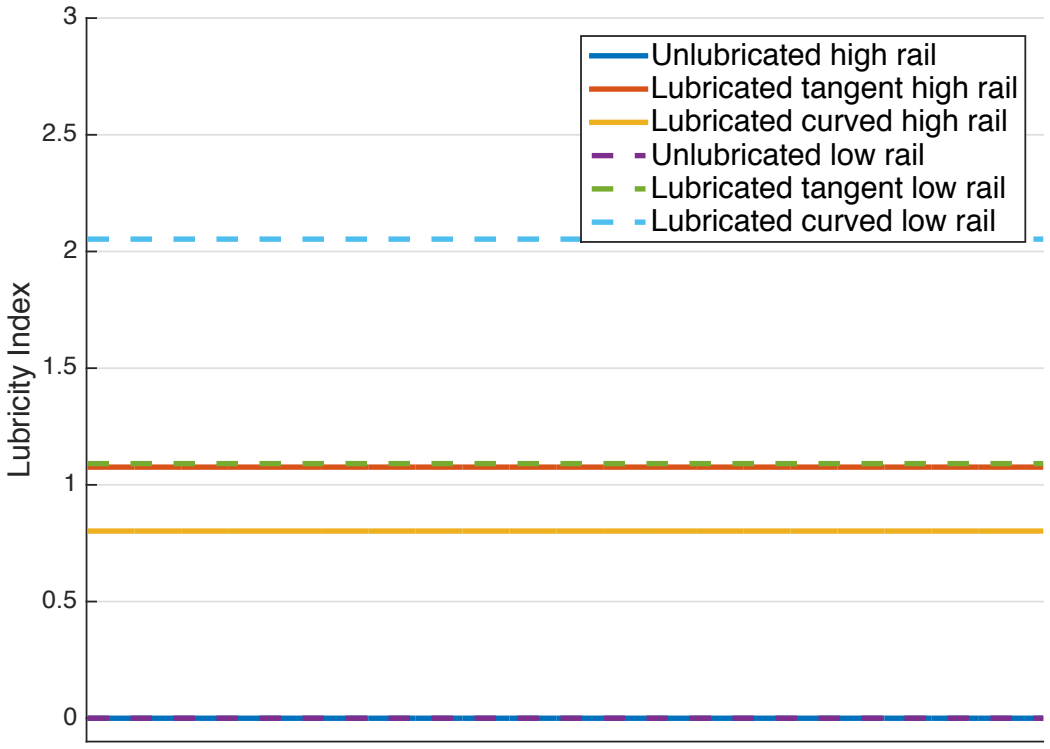

Figure 6-15 Lubricity index for southbound and northbound test sections

Chapter 7
System Parameters Effect

The effects of various system parameters are studied in this chapter. The parameters studied include lubricant layer thickness, laser sensor vibrations, and sensor angle (or angle of incident). For each parameter, tests are conducted in the laboratory, in the field, or in both, while changing each parameter individually. The test results are plotted similar to the earlier figures in order to assess the effect of each parameter.

7.1 Layer Thickness

Measuring lubricant layer thickness is as important to the railroad industry as detecting the lubrication. The lubricants are applied manually, using a paint roller. To achieve thinner layers, a dry roller is used to absorb some of the applied lubricant. Applying the dry roller in successive steps and making measurements in between each step allow us to collect data for various states of lubricity. Various tests with different quantities of lubricants, from very little to a significant amount, are performed, and the results are discussed for each lubricant separately.

7.1.1 Lubricant A

Lubricant A is tested both in the lab and in the field. Since this is a water-based lubricant, special care is taken to ensure that the lubricant does not excessively dry off in between the tests. The results shown in Figure 7-1 indicate that the laser system is able to correctly measure, qualitatively, the layer thickness as simulated by successively removing lubricant from the rail. It is important to note that although the results in Figure 7, which are filtered with moving average, do not provide an exact measure of how thin or thick the lubricant layer

is (say, in micrometers), they do indicate that the system output voltage increases according to decreasing lubricant layer thickness. A minimal amount of Lubricant A is close to unlubricated rail, but is still detectable.

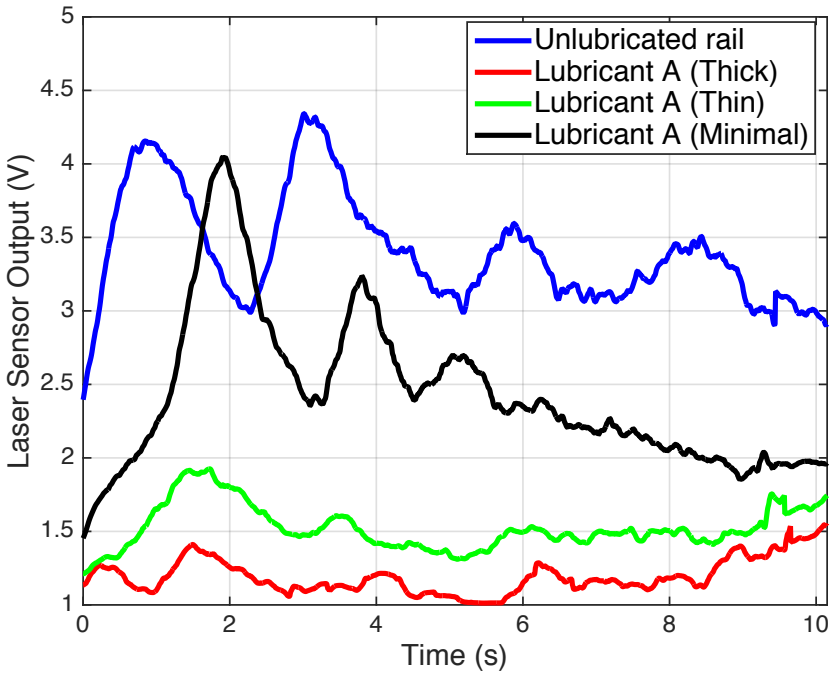

Figure 7-1 Specular reflection of different layer thicknesses of Lubricant A compared to unlubricated rail (Lab Track)

It is noted in the previous figure that at the 2-second mark, a higher signal for Lubricant A is obtained than that of the unlubricated rail. This is due to unsynchronized data. These tests are done separately, as mentioned earlier, and then processed to include all signals in the same time window. Thus, this peak at the Lubricant A signal represents the same area of the unlubricated rail at the 1.4-second mark. When comparing these two peaks, it is clear that the reflection value of Lubricant A is less that that of the unlubricated rail.

7.1.2 Lubricants B and C

Similar results are found for the two other lubricants; Figure 7-2 and Figure 7-3 plot the laser system output for different amounts of lubricants B and C, respectively. The changes in system output can be used to quantify the lubricant thickness, and to establish when the re-application of lubricant is needed.

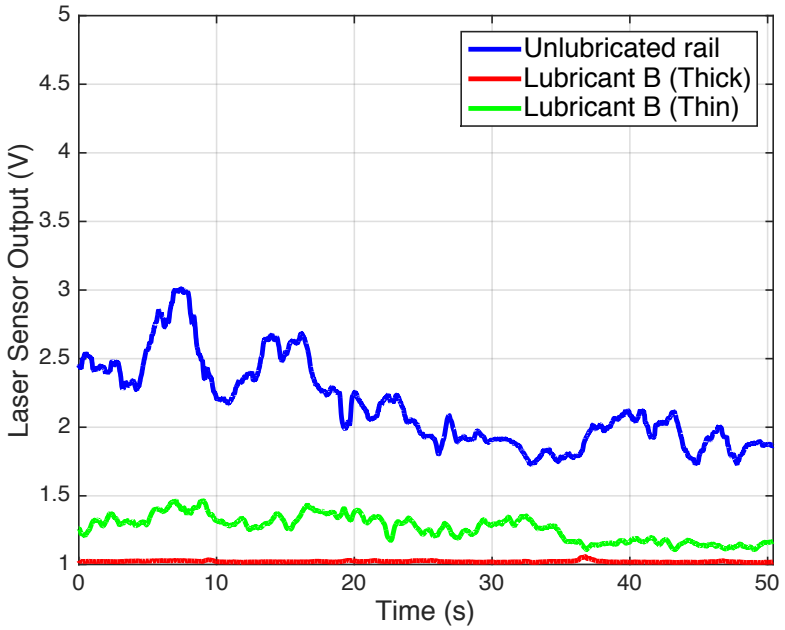

Figure 7-2 Specular reflections of different thickness layers of Lubricant B

When the lubricant gets too thin, the laser beam can partially penetrate the lubricant and reach the rail surface. This phenomenon causes the system readings to be similar to the readings for the unlubricated rail. This effect is obvious for lubricants A and C, however, it is not as obvious for lubricant B because of its considerably more opaque (black) state.

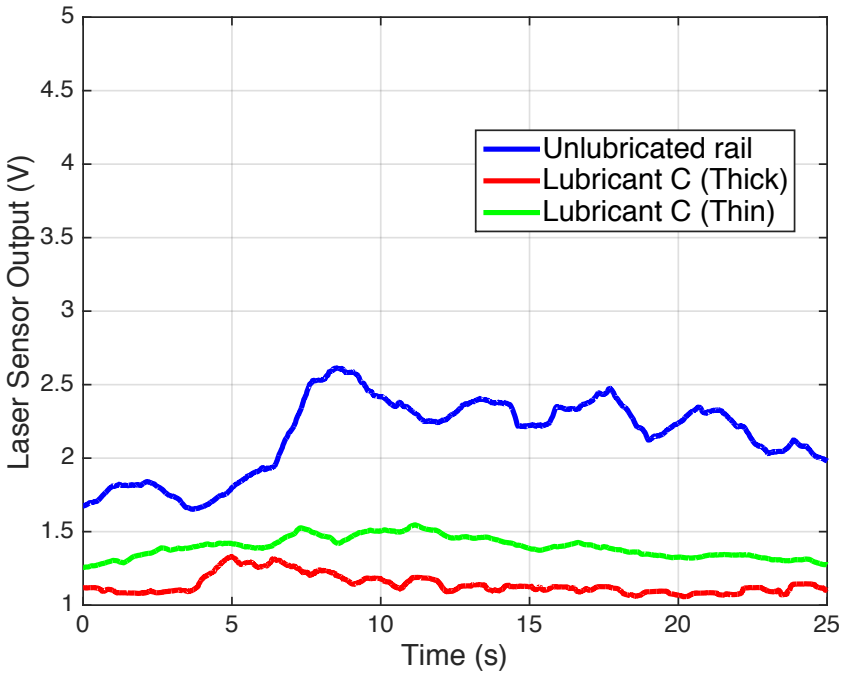

Figure 7-3 Specular reflections of different thickness layers of Lubricant C

7.2 Vibration and Motion

Studying the effect of vibration and motion on the results is important because the less sensitive to vibration the laser is, the more accurate the results will be. The tests presented in this section are performed in various dynamic conditions that are intended to assess whether the vibrations caused by the motion of the platform that carries the laser system affect its accuracy.

The setup used consists of three main parts: the laser, a piece of rail, and a vibration-simulating machine. A ROEHRIG Shock Dyno, shown in Figure 7-4, that vibrates with specified frequencies and amplitudes is used to simulate the rail/train vibration. The laser is fixed, while the piece of rail is vibrating.

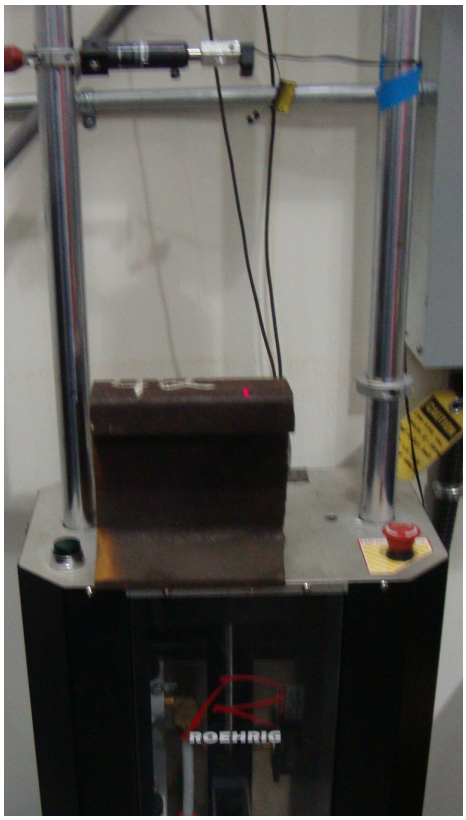

Figure 7-4 Vibration-simulating machine with installed laser system

The frequencies used in this test range from 0.5 Hz to 10 Hz. Moreover, amplitudes range from 0.5 inch to 3 inches. The tests are done with different combinations of the mentioned frequencies and amplitudes. The laser used in this test does not have an analog output, with only a digital display that shows the results. Because there is no way to collect the data from this laser, a comparison is made between all tests according to the voltage values shown in the digital display. Results are nearly identical, indicating that various vibration conditions do not influence test results.

To test the effect of lateral vibration on the results, a test was done and the results are presented. In this test, the cart was held stationary and restricted from movement in forward and backward directions, while forcing the laser head to move and vibrate laterally for about 15 degrees in each direction measured from the normal line. As shown in Figure 7-5, the lateral motion and vibration have minimal effect on the laser sensor output when compared to the effect of the lubrication. It is also worth mentioning that due to the cart stability and minimal

side-to-side motion, the lateral vibration that occurred in the field tests is much less compared to the test shown here. As a conclusion, the effect of lateral vibration does not influence test results and can be neglected, especially when compared to the effect of lubrication on the laser sensor outputs.

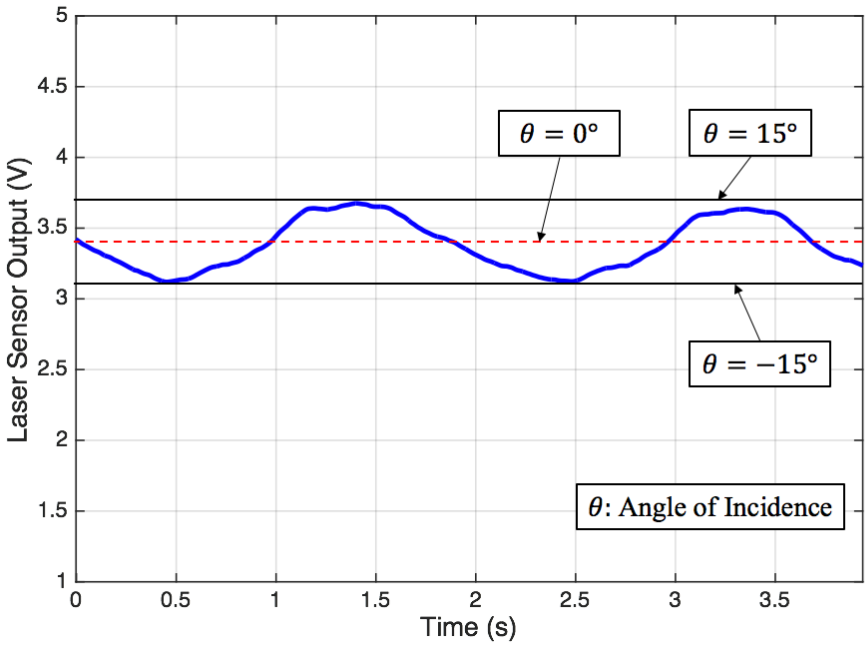

Figure 7-5 Effect of lateral vibration on laser sensor output

7.3 Ambient Luminance

The ability of the laser system to work in various ambient lighting conditions that are representative of the field environment is critical to its successful implementation for revenue service testing. The laser beam is visible and has a wavelength of 660 nm, which is in the visible range. According to the specification of the laser head (included in Appendix B.1), it has the capability to resist the effect of a wide range of operating ambient luminance, which ranges from an incandescent lamp of 10000 lux or less, to sunlight with 20000 lux or less.

To confirm, these tests were done with four different lighting conditions:

- normal indoor lighting,
- indoor with a bright 500-Watt light directly shining on the test area,
- outdoor with cloudy sky, and
- outdoor with direct sunlight.

The tests for various lighting conditions were performed identically to each other in order to maintain lighting condition as the only variable. As shown in Figure 7-6, the results for both lighting conditions, shaded and 500W light, are nearly identical, indicating that various lighting conditions do not influence the test results.

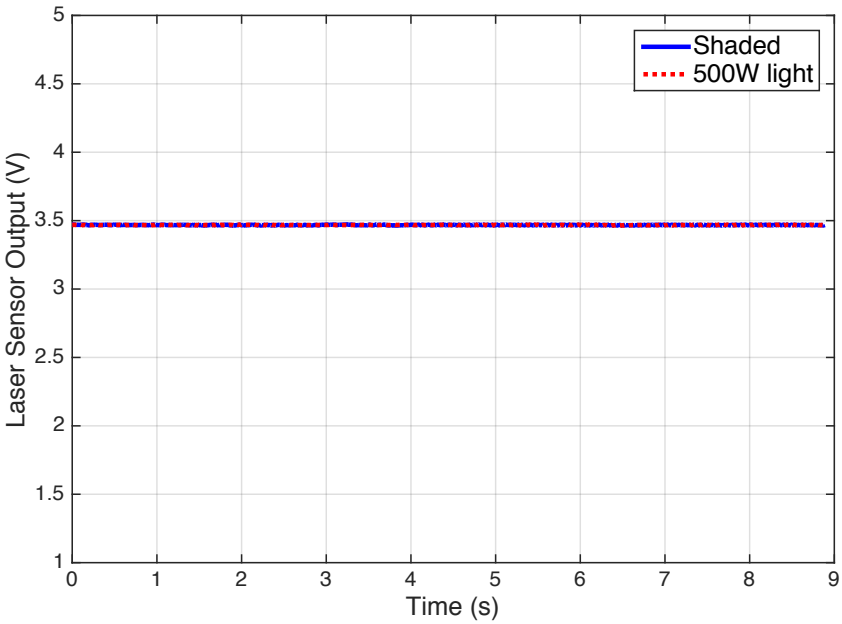

Figure 7-6 Laser sensor output of two different lighting conditions for the same spot

Often, one of the shortcomings of optical sensors is that they are sensitive to environmental lighting conditions, limiting their practical applications. The results in this section are quite significant in that they indicate that the lubricity sensor that is adapted for this study is impervious to the lighting conditions, and can be used in very low light to extremely bright lighting situations.

7.4 Angle of Incidence

To measure specular or diffuse reflections, angle of incidence is changed and modified accordingly. Figure 7-7 shows how diffuse reflection is measured and the beam is received from an uneven surface. The beam is scattered in all directions and the laser head receiver receives a fraction of that reflection.

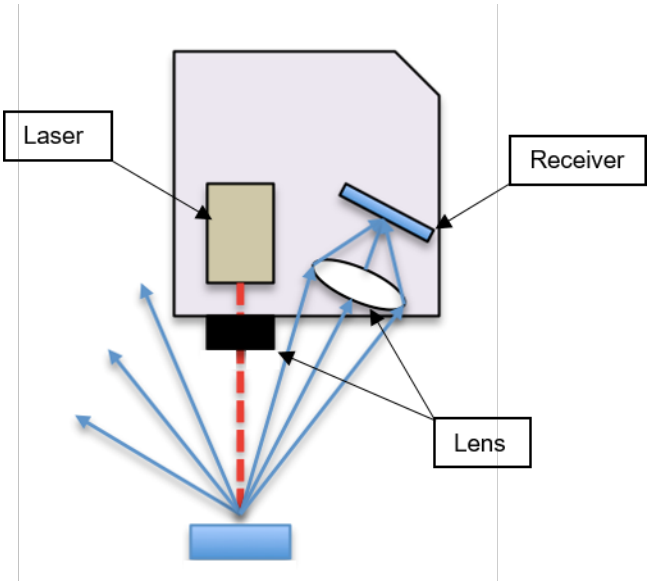

Figure 7-7 Sensor head setup for diffuse reflection of an uneven surface

For shiny surfaces like water, mirrors, or polished metal, the beam is reflected mostly in one direction. Figure 7-8 shows that if the laser beam is set up perpendicular to the test surface, then the reflected beam remains invisible to the receiver. Of course, such a setup would defeat the intended purpose of the sensor.

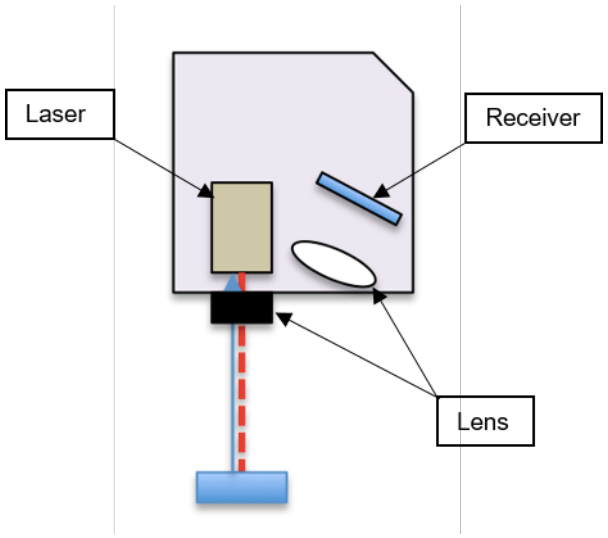

Figure 7-8 Sensor head with incorrect setup for specular reflection of a shiny surface

The proper setup of the laser beam involves a slight incident angle (say, in the range of 10 – 30 degrees) such that the reflected beams are visible by the receiver. As shown in Figure 7-9, the angle of beam incidence is the same as the angle of reflection because of the surface reflectivity.

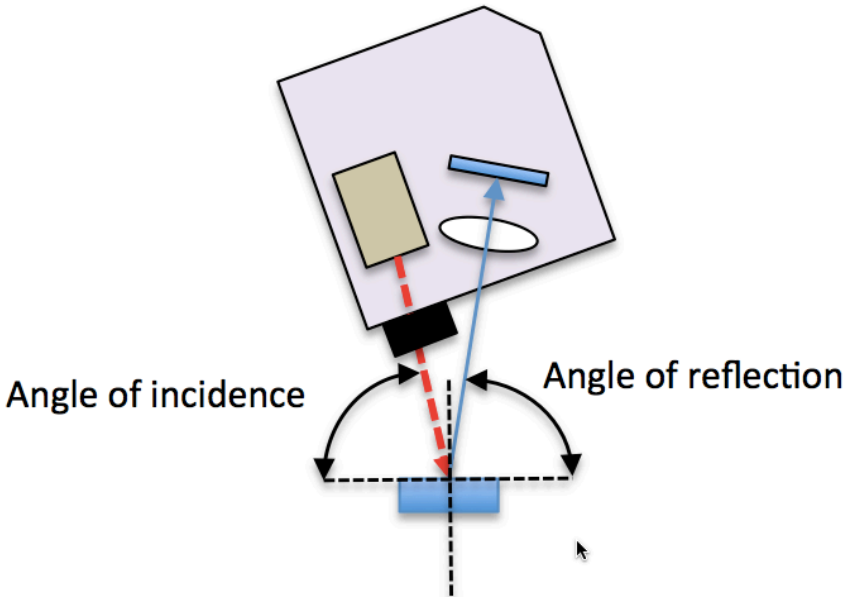

Figure 7-9 Sensor head adjustments for specular reflections of a shiny surface

Both specular and diffuse reflections are measured for the unlubricated rail and the lubricated surface. For a shiny surface, like an unlubricated rail surface, diffuse reflection is minimal compared to specular reflection. Thus, reduction in the reflection because of lubrication existence is barely noticeable. On the other hand, for a matte surface, diffuse reflection is much larger, and the difference between the unlubricated rail and the lubricated rail is high enough to be detected. Therefore, all tests in the previous sections and chapters were conducted considering specular reflection.

Chapter 8
Lubrication Quantification

This chapter presents various approaches and models to quantify lubricant monitoring results based on specular reflection measurements made by the laser measurement system. Different approaches to analyzing the measurement system's output are presented in order to quantify TOR lubricity, including the development of a Lubrication Index for numerically assessing the condition of the rail.

8.1 Boolean Assignment

When comparing the reflection of an unlubricated rail to itself after lubrication, the difference determines to what degree the rail is lubricated. The closer the reflection values are to each other, the dryer the rail will be. Each spot on the rail can be compared to itself before and after applying lubrication. This method, Boolean Assignment, will compare rail reflection point by point, and then combine the results of all points to determine a measure of the whole rail.

This approach works best with lubricants that have low reflection compared with an unlubricated rail, such as lubricants A and B. Every point scanned will be assigned a binary value: zero or one, which depends on its reflection value compared to one standard deviation below the unlubricated rail mean value. If the reflection value is higher, it will be assigned a new value of one. Otherwise, zero will be the new value. The mean of all points with their new values is then calculated and the percentage is proposed.

Figure 8-1 shows how specular reflection of Lubricant A is different and lower in value when compared with the unlubricated rail. In this case, the reflection voltages for Lubricant A are all lower than one standard deviation of the unlubricated rail. Therefore, 100% of the rail is

covered with Lubricant A. One standard deviation is used as an arbitrarily statistical value that can be increased or decreased according to more extensive field tests.

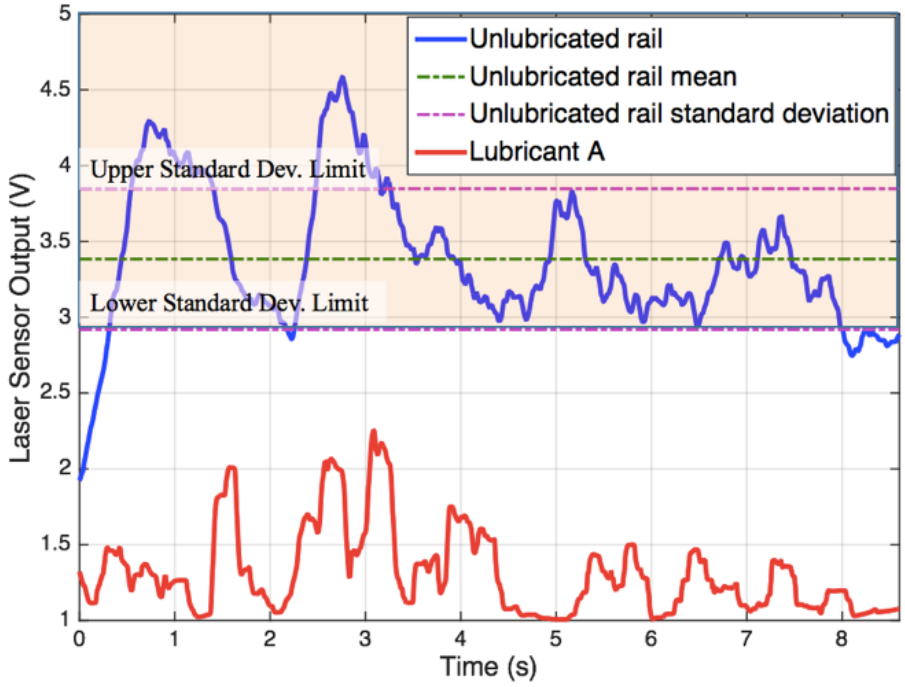

Figure 8-1 Unlubricated rail specular reflection with mean and standard deviation compared to Lubricant A

If the lubricant thickness layer is reduced to a lower level, certain locations on the rail would lose their lubrication, and for those, the measurements will fall above the lower standard deviation limit, as shown in Figure 8-2. In such case, the lubrication percentage will be less compared with the previous case, in which full lubrication exists. For this specific case, 81.6% of the points are below the lower standard deviation of the unlubricated rail, which represents 81.6% of lubrication coverage.

This method assumes that the cart is moving at a constant velocity. If it is not, then the distance should be used instead of time to calculate all averages and standard deviations. In that case, the cart is not required to move at a constant velocity.

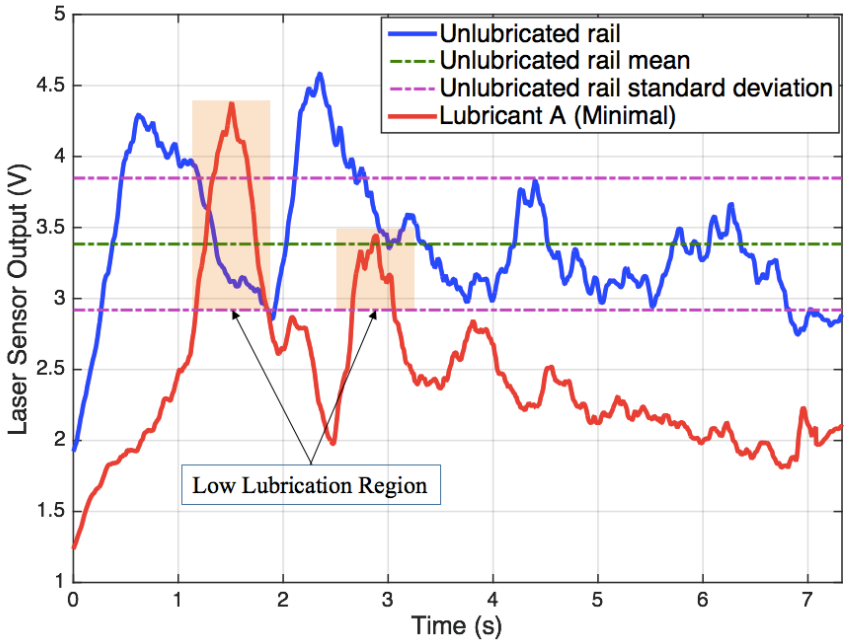

Figure 8-2 Unlubricated rail specular reflection with mean and standard deviation compared to minimum amount of Lubricant A

On the other hand, this approach does not provide an accurate result with transparent lubricants like Lubricant C. Lubricant C has the highest specular reflection values compared to all other lubricants. Hence, using this approach may lead to some confusion. Figure 8-3 shows that some of the Lubricant C reflection values are above the lower standard deviation of the unlubricated rail, however, Lubricant C covered 100% of the rail total area. According to this approach, lubrication coverage area equals 59.8%.

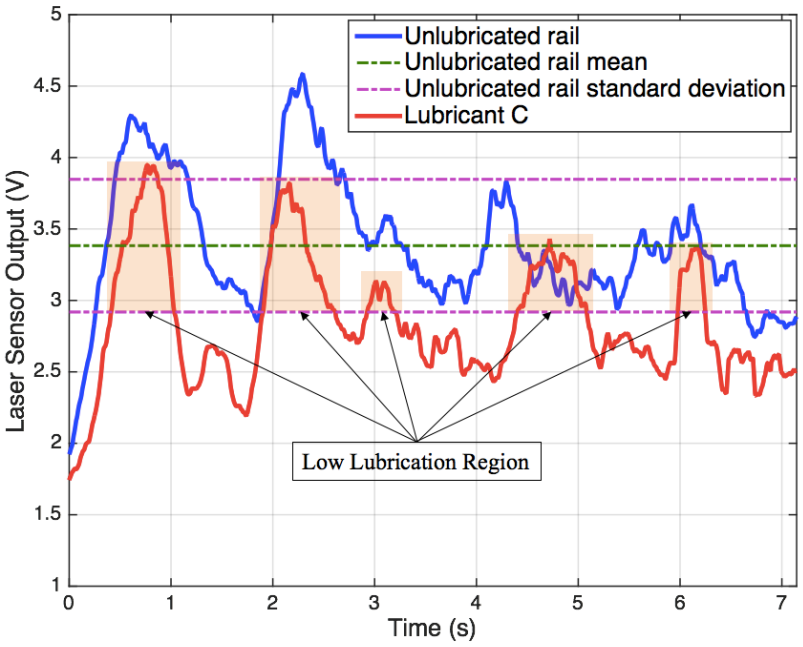

Figure 8-3 Unlubricated rail specular reflection with mean and standard deviation compared to Lubricant C

The results in Figure 8-3 indicate the need for a more capable and sophisticated approach to quantifying the lubricity of the rail.

8.2 Lubrication Index

This approach depends on the mean value of lubricant reflection, and a subsequent comparison to the mean and standard deviation (Figure 8-4) of the unlubricated rail according to:

$$\ell = \begin{cases} \dfrac{\overline{D} - \overline{L}}{\sigma_D}, & (\overline{D} - \overline{L}) > \sigma_D \\ 1, & (\overline{D} - \overline{L}) \leq \sigma_D \end{cases} \tag{8-1}$$

where ℓ is the Lubrication Index, $\overline{D}$ and $\overline{L}$ are mean reflection values of the unlubricated rail and lubricant, respectively, and σ_D is the standard deviation of the unlubricated rail reflection. The closer the index is to one, the larger the rail segment that is covered with lubrication.

Conversely, the closer the index is to zero, the less lubricated is the rail segment. Values higher than one are considered equal to one.

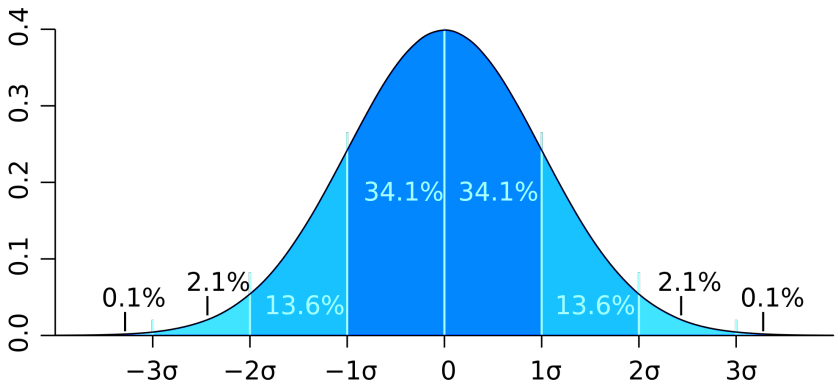

Figure 8-4 Mean and standard deviations in normal distribution

Figure 8-5 shows how the mean value of Lubricant C is below the mean value for the unlubricated rail minus one standard deviation, which makes the difference $(\overline{D} - \overline{L})$ higher than the unlubricated rail standard deviation σ_D. Hence, Lubrication Index ℓ will be greater than one, which means the rail is completely lubricated.

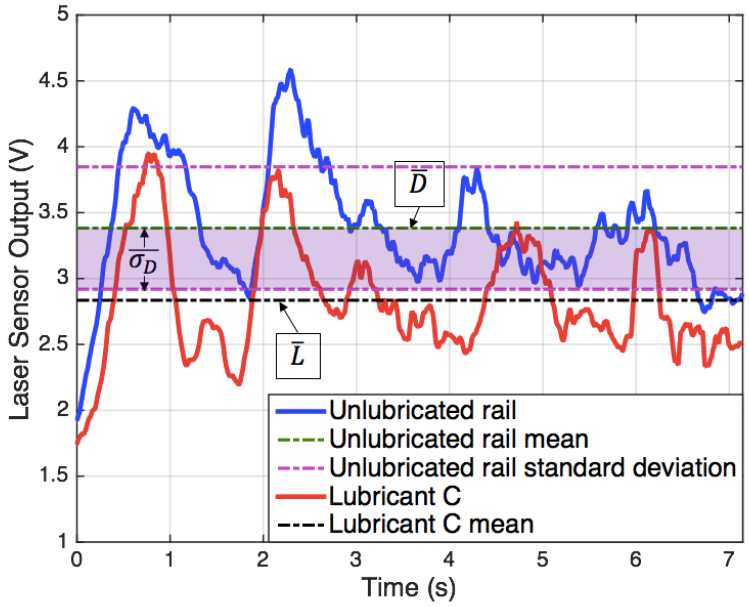

Figure 8-5 Comparison between Lubricant C and unlubricated rail mean values

This index works accurately for small segments, but higher deviations of lubricant reflection will reduce the accuracy of this index. Thus, it is recommended that this index be used for small segments of rail, with the following calculation used to determine the overall index for a large section:

$$\bar{\ell} = \frac{\sum \ell_i x_i}{\sum x_i} \tag{8-2}$$

where $\bar{\ell}$ is the Overall Lubrication Index, i is segment number, x_i is the length of the i^{th} segment, and ℓ_i is the Lubrication Index of the i^{th} segment.

This approach provides a more accurate method to quantify rail lubrication compared with the earlier method. However, it requires a higher sampling rate to process the data represented by small segments. Shorter segments are results in a more accurate rail lubrication index. The laser used for the tests shown in previous chapters has a high sampling rate that makes it capable of collecting data for short rail segments.

Chapter 9
Conclusions and Future Work

9.1 Summary and Conclusions

Detecting rail lubrication in an accurate way is an issue that needs to be addressed in the railroad industry. Improper inspection frequency leads to either higher maintenance cost and/or potentially excessive rail wear and tear. Traditional lubrication techniques are highly subjective, mostly depending on the trained eyes of rail engineers and their field experience. In order to improve the accuracy and dependability of rail lubricity measurements, methods that can provide a direct and accurate assessment of the degree of lubrication of a rail are needed.

A laser-based sensor technology is proposed to detect, measure, and monitor the condition of rail TOR lubricants. A large number of tests are performed to verify the concept in various settings, including a track panel at the Railway Technologies Laboratory of Virginia Tech, on a section of yard rail, and on revenue-service track. Three different lubricants commonly used by the U.S. railroads were considered for the study. The parameters that could affect the practical implementation and application of the measurement system were studied in order to assess any errors that may be introduced in the measurements while using the system in revenue service under moving condition. In addition to reporting on the system's ability to qualitatively measure the extent of rail lubrication, an attempt was made at introducing quantitative measures that could be used for assessing rail lubrication in an indexed manner. To this end, three models were proposed to quantify results.

Based on the results of the tests performed during this study, the following conclusions can be made:

- The laser-based sensor is capable of detecting the existence of rail TOR lubricants with high precision. Specular reflection is measured on the unlubricated rail and compared with the lubricated rail. A lubricated rail reflects less light compared with an unlubricated rail due to the absorption (less reflection) of light that occurs when lubricants are present on the rail.
- Various lubricants have different characteristics which affect the laser system's measurements. The oilier the lubricant is (like Lubricant C), the more difficult it is to detect because of its high reflectance of light when compared with water-based lubricants.
- Lubricant layer thickness is inversely proportional to the amount of light reflected. In other words, the more lubricated the rail surface is, the less it reflects light.
- The laser sensor is able to detect a large range of lubricant thicknesses, from an almost invisible thin layer, to a heavily-applied thick layer.
- Among the parameters that can affect the system performance, vibrations, ambient lighting, and angle of incidence are evaluated individually. None of these environmental factors had any effect on the accuracy of the measurements, or on the ability of the system to detect lubricity. It is worth noting that all of the measurements presented in this study were made at low (walking) speeds. The ability of the system to perform at higher speeds (say, in the range of 20 to 100 mph) was not studied. It is expected, however, that the system will perform in a satisfactory manner at train operating speeds, although such tests must be performed in the future.
- The effect of light angle of incidence is an essential factor in the field implementation of the laser system. In order to enable the system to differentiate between unlubricated and lubricated rails with a higher degree of accuracy, specular reflection is considered in favor of diffuse reflection. Specular reflection is found to provide higher sensitivity to the presence or absence of TOR lubricants, making it easier to detect them.
- Three different models, theoretical and empirical, are proposed to quantify the results. Each model has its own pros and cons that can affect its ability to quantify TOR lubricants based on the length of rail section, preparation time, rail availability, and transparency of the lubricant.

9.2 Future Work

- The utilization of the developed system for optimizing TOR friction modifiers is recommended for future studies. Examples of the applications the can utilize the TOR lubrication detection system include:
    - Optimizing fuel efficiency
    - Optimizing lubricant and rail inspections
    - Reducing train lateral forces
    - Reducing rail and wheel wear
    - Improving braking practices in PTC

- Different quantification methods can be developed using laser technology to assess, detect, and measure rail lubrication conditions. Unlike the approaches presented in the previous chapter to quantify the rail lubrication condition, this approach depends on the direct impact of lubrication on train lateral forces. The idea behind this approach is to correlate specular reflection signals with their effect on lateral forces of the train passing by. One of the main advantages of this approach is that it directly relates specular reflection measurements to an important parameter (lateral forces) in the railroad industry. Lateral force is the main parameter that allows the railroad to determine the need of lubrication: higher lateral forces result in decreased safety and efficiency. In addition, high lateral forces have a negative effect on rail and wheel wear, as mentioned earlier.

References

[1] M. El-Sibaie, D. Jamieson, B. Mee, B. Whitten, K. Kesler, D. Tyrell and J. Dorsey, "Engineering studies in support of the development of high-speed track geometry specifications," in *IEEE/ASME Joint Railroad Conference*, Boston, Massachusetts, 1997.

[2] C. Esveld, "Modern railway track," 2001.

[3] G. W. J. Heynen, "Railway induced vibrations," 1987.

[4] A. B. Stanbridge and D. J. Ewins, "Measurement of translational and angular vibration using a scanning laser Doppler vibrometer," *Shock Vib.,* vol. 3, no. 2, pp. 141-152, 1996-1997.

[5] Kim, Dongkyu, H. Song, H. Khalil, J. Lee, S. Wang and K. Park, "3-D Vibration Measurement Using a Single Laser Scanning Vibrometer by Moving to Three Different Locations," *IEEE Transactions on Instrumentation and Measurement,* vol. 63, no. 8, pp. 2028-2033, 2014.

[6] Krause, Hans and H. Lehna, "Investigation of tribological characteristics of rolling-sliding friction systems by means of systematic wear experiments under well-defined conditions," *Wear,* vol. 119, no. 2, pp. 153-174, 1987.

[7] K. Davis, "Evaluation of a top-of-rail lubrication system," in *U.S. Dept. of Transportation, Federal Railroad Administration, Office of Research and Development*, Washington, DC, 1999.

[8] "TTC Technical Note," in *TTC-006 (FAST-TN84)*, February 17, 1984.

[9] R. Reiff, "Rail/wheel lubrication studies at FAST," *Lubr. Eng.,* vol. 42, pp. 340-349, 1986.

[10] J. M. Samuels and D. B. Tharp, "Reducing Train Rolling Resistance by On-Board Lubrication," in *2nd Rail and Wheel Lubrication Symposium*, Memphis, USA, 1987.

[11] G. Dahlman and M. Stehly, "Energy savings from rail lubrication on the Santa Fe Railway," in *Proc. Symp. on Rail and Wheel Lubrication*, Memphis, TN, 1987.

[12] J. Dearden, "The wear of steel rails and tyres in service," *Wear,* no. 3, pp. 43-59, 1960.

[13] J. Dearden, "The wear of steel rails: a review of the factors involved," in *Proc. Inst. Civil*

Eng., London, May 1954.

[14] R. P. Reiff, S. Gage and S. Kumar, "TOP-OF-RAIL LUBRICATION ENERGY TEST," in *U.S. Department of Transportation Report Number DOT/FRA/ORD-98/01*, February 1998.

[15] S. Kumar, C. G., V. Reddy and U. Kumar, "Issues and challenges with logistics of rail maintenance," in *Proceedings of the Second International Logistics Sections Conference*, 2006.

[16] R. Fröhling, J. De Koker and M. Amade, "Rail lubrication and its impact on the wheel/rail system," *Proceedings of the Institution of Mechanical Engineers, Part F: Journal of Rail and Rapid Transit,* vol. 223, no. 2, pp. 173-180, 2009.

[17] A. J. Peters and R. P. Reiff, "SUMMARY OF WHEEL RAIL LUBRICATION RESEARCH," in *No. FORMAL REP.*, 1989.

[18] R. G. Gould, "The LASER, Light Amplification by Stimulated Emission of Radiation," in *Franken, P.A. and Sands, R.H. (Eds.). The Ann Arbor Conference on Optical Pumping, the University of Michigan*, 1959.

[19] S. Crouch and D. A. Skoog, Principles of instrumental analysis, Thomson Brooks/Cole, 2007.

[20] American National Standards Institute (ANSI), Thermal insulation - Heat transfer by radiation - Physical quantities and definitions, 1989.

[21] S. Juds, "Photoelectric sensors and controls: selection and application," *CRC Press,* vol. 63, 1988.

[22] P. Kubelka, "The kubelka-munk theory of reflectance," *Z Tech Phys,* vol. 12, p. 539, 1931.

[23] E. Hecht, Optics (4th ed.), Addison Wesley, 2002.

[24] W. West, Absorption of electromagnetic radiation, AccessScience. McGraw-Hill.

[25] J. Watkinson, The Art of Sound Reproduction, Focal Press, 1998, pp. 268, 479.

[26] J. Dongarra and F. Sullivan, "Guest Editors Introduction to the top 10 algorithms," *Computing in Science Engineering,* vol. 2, no. 1, pp. 22-23, January 2000.

Appendix A

Lubricants Specification

A.1 Lubricant A

Table A−1 Lubricant A specification

Formulation Options	Freight / Transit
Fire Safety	Non-Flammable
Odor	Slight Odor
Freezing Point (C^o)	-6 (-16) Freight (LT) / -6 (Transit)
Viscosity, cP at 25^oC	22,700-24,700 (17,000-19,000) Freight (LT)
Friction Levels	0.30 to 0.40 μ
Carry Distances	1 to 2 miles
Application Rate	0.5 L/1000 axles

A.2 Lubricant B

Table A−2 Lubricant B specification

Physical State	Solid [Paste]
Color	Black
Odor	Mild
pH	7.5
Flash Point	$> 204^oF$
Relative Density	1.3
Chemical Stability	Stable
Usable Temperature Range	$10^o$to 140^o

A.3 Lubricant C

Table A−3 Lubricant C specification

Color	Clear
Odor	Odorless
Water Solubility	Non-soluble
Application Method	Spray
Physical Viscosity	Viscous, oily liquid
Ideal Climate	Hot/Cold, dry/wet
Minimum Pour Point	$-40^{o}\mathrm{F}$
Ideal Gravity	0.85 to 0.89

Appendix B
Laser Specifications

B.1 Sensor Head Specification: LV-NH32

Table B−1 Sensor head specification (LV-NH32)

Type		Adjustable spot type	Coaxial reflective type	Super small spot type	Wide area reflective type	Coaxial retro-reflective type	Area thrubeam type		
Model		LV-NH32	LV-NH35	LV-NH37	LV-NH42	LV-NH62	LV-NH100	LV-NH110	LV-NH300
Laser class	FDA (CDRH) Part1040.10	Class 1 laser product							
	IEC 60825-1	Class 1 laser product							
Light source		Visible light semiconductor, laser wavelength: 660 nm, output: 310 µW							
Detection distance (mm)	MEGA	1200	750	70 ± 15	1200	8000	2000 (detection width10 mm)		2000 (detection width 30 mm)
	ULTRA	1000	600		1000	7000			
	SUPER	750	450		750	6000			
	TURBO	500	300		500	5000			
	FINE	250	150		250	3500			
	HIGH SPEED	200	100		200	2000			
Beam spot size		ϕ0.8 mm or less at detection distance up to 300 mm	Approx. ϕ2 mm at detection distance up to 600 mm	Approx. ϕ50 µm at the detection distance 70 mm	Area width approx. 37 mm at detection distance 150 mm (Black slit: approx. 19 mm) (Gray slit: approx. 7 mm) Thickness: 1 mm or less	Approx. ϕ1.5 mm (Detection distance 1 m or less)	Area width approx. 12 mm		Area width approx. 32 mm
Indicator		Laser transmission warning lamp: Green LED Level indicator: Green × 2, red × 1 (Level indicator shows detection margin 90 to 110%)					Laser transmission warning lamp, power indicator (only receiving part): Green LED Level indicator: Green × 2, red × 1 (Level indicator shows detection margin 90 to 110%)		
Environmental resistance	Operating ambient luminance	Incandescent lamp: 10,000 lx or less; sunlight: 20,000 lx or less							
	Ambient temperature	- 10 °C to + 55 °C (no freezing)							
	Relative humidity	35 to 85% RH (no condensation)							
	Vibration	10 to 55 Hz, compound amplitude 1.5 mm, 2 hours for each of X, Y, Z axes							
	Shock resistance	Shock resistance 500 m/s^2, 3 times for each X, Y, Z axis direction							
Material	Housing	Glass-reinforced resin							
	Lens cover	Transmitter: Acrylic Receiver: Polyarylate	Norbornene resin	Transmitter: Glass Receiver: Polyarylate	Polyarylate	Norbornene resin	Transmitter: Glass Receiver: Polyarylate		
	Cable	PVC							
	Accessories	Mounting bracket: SUS304	Mounting bracket: SUS304	Mounting bracket: SUS304	Slit: Polyacetal Mounting bracket: SUS304	Reflector: Acrylic resin, polycarbonate Mounting bracket: SUS304	–		
Weight		Approx. 65 g	Approx. 65 g	Approx. 65 g	Approx. 65 g	Approx. 65 g	Approx. 75 g	Approx. 75 g	Approx. 95 g

B.2 Sensor Amplifier Specification: LV-N11MN

Table B−2 Sensor amplifier specification (LV-N11MN)

Type		2 output		1 output		0-line	Monitor output
Cable / Connector		Cable		M8 connector		–	Cable
Main unit / Expansion unit		Main unit	Expansion unit	Main unit	Expansion unit	Expansion unit	Main unit
Model	NPN	LV-N11N	LV-N12N	LV-N11CN	LV-N12CN	LV-N10	LV-N11MN
	PNP	LV-N11P	LV-N12P	LV-N11CP	LV-N12CP		–
Input/output	Control output	2 output		1 output		N/A	1 output
	External input	1 input		1 input		N/A	1 input
	Monitor output	N/A					1 output
Response time		80 µs (HIGH SPEED) / 250 µs (FINE) / 500 µs (TURBO) / 1 ms (SUPER) /4 ms (ULTRA) / 16 ms (MEGA) * 80 µs cannot be selected when LV-S31 / S62 / S63 is connected.					
Output operation		Light-ON / Dark-ON switch					
Timer function		Timer OFF, OFF delay, ON delay, One-shot Timer variable (1 ms to 9999 ms) Maximum error to setting value is ± 10% or less					
Control output	NPN output	NPN open collector 30 V, Residual voltage 1 V or less (Output current: 10 mA or less) / 2 V or less (Output current: 10 to 100 mA) (Stand-alone) 1 output max: 100 mA or less, 2 output total: 100 mA or less (Multiple connections) 1 output max: 20 mA or less					
	PNP output	PNP open collector 30 V, Residual voltage 1.2 V or less (Output current: 10 mA or less) / 2.2 V or less (Output current: 10 to 100 mA) (Stand-alone) 1 output max: 100 mA or less, 2 output total: 100 mA or less (Multiple connections) 1 output max: 20 mA or less					
Monitor output (Only LV-N11MN)		Voltage output: 1 to 5 V, load resistance: 10 kΩ or more, repeat accuracy: ± 0.5% of F.S. Response time: 1ms (HIGH SPEED / FINE / TURBO),1.2 ms (SUPER), 1.8 ms (ULTRA), 4.2 ms (MEGA)					
External input		Input time 2 ms (ON) / 20 ms (OFF) or more [*1]					
Expansion units		Up to 17 units can be connected in total. (The 2-output type is treated as 2 units.)					
Protection circuit		Protection against reverse power connection, output overcurrent, and output surge					
Number of interference prevention units	Connect with other than LV-S31	HIGH SPEED: 0, FINE / TURBO / SUPER: 2, ULTRA / MEGA: 4 (These numbers double when "Double" is selected.)					
	Connect with LV-S31	FINE: 2, TURBO / SUPER / ULTRA / MEGA: 4 (These numbers double when "Double" is selected.)					
Rated	Power voltage[*4]	24 VDC (operating voltage 10 to 30 VDC (including ripple)), ripple (P-P) 10% or less, Class 2 or LPS [*6]					
Rated	Power consumption[*5] NPN	Normal: 830 mW or less (at 30 V. 30 mA at 24 V, 56 mA or less at 12 V)[*2] Eco on: 710 mW or less (at 30 V. 26 mA at 24 V, 48 mA or less at 12 V)[*2] Eco full: 550 mW or less (at 30 V. 21 mA at 24 V, 40 mA or less at 12 V)					
Rated	PNP	Normal: 950 mW or less (at 30 V. 33 mA at 24 V, 60 mA or less at 12 V)[*2] Eco on: 815 mW or less (at 30 V. 29 mA at 24 V, 52 mA or less at 12 V)[*2] Eco full: 650 mW or less (at 30 V. 24 mA at 24 V, 40 mA or less at 12 V)				–	
Environmental resistance	Ambient temperature	- 20 °C to + 55 °C (no freezing)[*3]					
	Relative humidity	35 to 85% RH (no condensation)					
	Vibration	10 to 55 Hz, compound amplitude 1.5 mm, 2 hours for each of X, Y, Z axes					
	Shock resistance	500 m/s^2, 3 times for each X, Y, Z axis direction					
Material	Housing	Amplifier body and dust cover material: Polycarbonate					
	Cable	PVC					
Housing dimensions		H 32.6 mm × W 9.8 mm × L78.7 mm					
Weight		Approx. 75 g	Approx. 65 g	Approx. 20 g	Approx. 20 g	Approx. 20 g	Approx.75 g

*1 : The input time is 25 ms (ON) / 25 ms (OFF) only when external calibration input is selected.

*2 : Increases 30 mW (1 mA) for HIGH SPEED Mode

*3 : When expanding, always install on a DIN rail (installed on the metal plate), and keep the output current to 20 mA / unit or less. When expanding units, the working ambient temperature will change according to the following conditions:1 or 2 units connected: - 20 to + 55 °C; 3 to 10 units connected: - 20 to + 50 °C; 11 to 16 units connected: - 20 to + 45 °C. When using the 2 output type, one unit is counted as 2 units.

*4 : When connecting 9 or more expansion units, ensure that the power voltage is 20 V or more.

*5 It increases by 15% when connected to the LV-NH100/NH110/NH300. It does not include the power consumption of the load. Power consumption when expansion units are connected is the total power consumption of each amplifier unit. Example: When one main unit (LV-N11N) is connected to 2 expansion units (LV-N12N) and they are used with LV-NH100 heads in HIGH SPEED mode. (1.15860 mW 1) + (1.15860 mW 2) = max. 2967 mW

*6 : Use with the over current protection device which is rated 30 V or more and not more than 1 A.

B.3 Monitor Output Type Input/Output Circuit Diagram

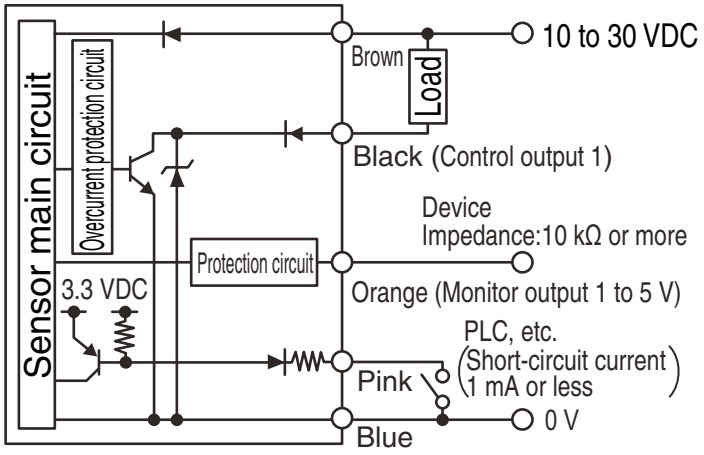

Figure B−1 Monitor output circuit diagram